UNIVERSITY OF THE
WITWATERSRAND,
JOHANNESBURG

THE EFFECT OF FLY ASH TYPE ON CEMENT PROPERTIES FOR OIL WELL DRILLING PURPOSES

MSc (50/50) RESEARCH REPORT

Prepared by

Zoë Betty Panda

(514636)

Submitted to

School of Chemical and Metallurgical Engineering, Faculty of Engineering and the Built Environment, University of the Witwatersrand, Johannesburg, South Africa

Supervisor: Dr Diakanua Nkazi

Co-supervisor: Prof Jeremy Gaylard

July 2020

ACKNOWLEDGEMENT

My wholehearted gratitude to God Almighty, the creator of heaven and earth for making the impossible possible!

I want to thank my mum Celestine and pay special tribute to my late dad Jean Pierre Fesele Panda for their guidance, moral and financial support. I am sure my dad would have beamed with pride had he lived to see this day! A special tribute goes also to my late aunt Albertine Panda for her contribution, support, inspiring me to always pursue excellence and her positive attitude toward my studies.

To my love Emmanuel, thank you for your support in the avenues of my life. To my entire family, thank for your patience, unconditional love and support throughout this journey.

I sincerely wish to thank Professor Herman Potgieter for giving me the opportunity and the continued support without which it would not have been possible to complete this project.

My heartfelt gratitude goes to my supervisor Dr Diakanua Nkazi without whom this research could not have been possible. Thank you for giving me the opportunity to learn and apply myself in a field that was once foreign to me. Your financial support has been remarkable. To Professor Jeremy Gaylard, thank you for your continued support and in-depth unique contribution throughout the duration of this research. A special thanks go to the following companies and individuals:

Chemical Industries Education and Training Authorities (CHIETA) for proving me with the much-needed funding which enabled me to accomplish this work.

Lafarge for giving me access to all the necessary resources and laboratory space to carry out my cement and fly ash tests. Particularly, I would like to thank Wilson Nala (Cement specialist) for his assistance in running the test and conducting the experiment. Bethuel Masedi (Lab Tester) for his assistance with the compressive strength testing of samples. Ntabiseng (Quality Assurance Analyst) for assistance with the chemical analysis. Antofogasta Mokoena (Chemical Analyst) for assisting with the chemical analysis. Dr Mike Otieno for his input in the early phase of my research. Banele Qumba (Technical Assistance) for his assistance with equipment and cement quantity determination. Petra Dinham for her assistance with SEM & XRD. Janet Smith for her assistance with XRD. Paul Den Hoed and Ben-Louis Van der Walt for their assistance with the temperature log.

PPC for providing me with the much-needed oil well cement equivalent to conduct my experiments.

Sika for providing me with the required retarder to conduct the experiment.

The Department of Chemical and Metallurgical Engineering (CHMT) and School of Civil and Environmental Engineering at the University of the Witwatersrand, including the staff and fellow students. I acknowledge all the drivers, technicians, secretaries, and personnel in the department who contributed directly and indirectly to this work.

Table of Contents

LIST OF FIGURES

LIST OF TABLES

NOMENCLATURE

	Chemistry Notation	Cement Chemistry Notation
Tricalcium silicate (Alite)	$3CaO.SiO_2$	C_3S
Aluminium oxide	Al_2O_3	A
Dicalcium silicate (Belite)	$2CaO.SiO_2$	C_2S
Calcium oxide	CaO	C
Calcium Silicate Hydrate	$3CaO.2SiO_2.3H_2O$	C-S-H
Calcium hydroxide	$Ca(OH)_2$	CH
Carbon Dioxide	CO_2	
Hydrogen Sulfide	H_2S	
Iron (III) oxide	Fe_2O_3	F
Silicon dioxide	SiO_2	S
Tetra calcium aluminoferrite	$4CaO.Al_2O_3.Fe_2O_3$	C_4AF
Tricalcium aluminate	$3CaO.Al_2O_3$	C_3A
Water	H_2O	H

Description	Abbreviations
American Petroleum Institute	API
American Society for Testing and Materials	ASTM
Bearden units of consistency	Bc
Bottom-hole circulating temperature	BHCT
Fly Ash	FA
High Pressure High Temperature	HPHT
Kilopascal	kPa
Lignosulphonate mid-range water reducing admixture	LSM
Loss on Ignition	LOI
Megapascal	MPa
Oil well cement	OWC

Pretoria Portland Cement	PPC
Researchers at King's College London	KCL
Scanning electron microscopy	SEM
Supplementary cementitious materials	SCM
Thermogravimetric analysis	TGA
Ultra High Performance Fibre Concrete	UHPFC
Wait-On-Cement	WOC
Water-to-cement ratio	w/c ratio
X-ray Fluorescence	XRF
X-ray powder diffraction	XRD

OIL DRILLING TERMINOLOGY

Float collar: is a part near the bottom of the casing string which catches the bottom and the top plugs, and which prevents mud from entering the casing (Glossary, 2014).

Guide shoe: a bull-nose shaped device attached to the bottom of the casing string. It allows the casing to be suspended from the wellhead (Glossary, 2014).

Cementing head: it is used to introduce and separate fluid in a well. The cementing head includes a plug container that has upper and lower fluid inlets oriented tangentially to the bore of the plug container (Glossary, 2014).

Pozzolanic: is by definition a material capable of binding calcium hydroxide in the presence of water (Glossary, 2014).

Wellbore: a drilled hole for exploration purposes and recovery of natural resour0ces including water, gas or oil, gas (Glossary, 2014).

	MEASUREMENTS UNITS
Shear rate	$\mathbf{s^{-1}}$
Viscocity	cP

OIL WELL CEMENT GRADES

Ordinary	O
Medium sulfate-resistant	MSR
High sulfate-resistant	HSR

FLY ASH AND CEMENT TERMINOLOGY

Cenosphere: hollow particles of FA with density less than 1.0 g cm-3, largely of silica and aluminium (Yoriya, et al., 2019); (Matsunaga, et al., 2001).

Dura-Pozz: A classified FA (size grading 90% - 45 µm) used as a cement extender and which is the highest quality processed ash in South Africa that conforms to international standards SANS50450 (Heyns & Hassan, 2009).

Plerospheres: are particle of hollow and generally thin-walled spherical FA, comprising of a number of the smaller FA particles of various size (mainly <10 µm) (F.Goodarzi & H.Sane, 2009).

Pozz-Fill: Unclassified FA (size grading -120 µm) used by blenders as an extender for cement in certain applications. Pozz-Fill only conforms to certain international standards. However, it has successfully been utilized for cement production in South Africa (Heyns & Hassan, 2009).

Super-Pozz: Classified FA (size grading 90% - 11 µm) with a mean particle diameter ranging from 3.9 to 5.0 µm. Super-Pozz is known for reducing water in the mixture and enhanced strength, for a given workability (Summers, 2004).

False set: This phenomen occurs when improperly stored cement contains C_3A of low reactivity and a large proprtion of more soluble calcium sulphate hemihydrate (Bapat, 2012).

Flash set : It occurs when cement contains high proportion of reactive C_3A but the souble content is less than that required for normal hydration (Bapat, 2012).

ABSTRACT

The critical steps that oil well cement (OWC) plays in drilling make oil well cementing arguably the most important operation performed on a well. The aim of this research was to assess the effect of coal fly ash (FA) on class G oil well cement FA (metal oxides, Loss on Ignition (LOI), morphology, particle size distribution) was characterised using X-ray Fluorescence (XRF), X-ray Diffraction (XRD), Scanning Electron Microscopy (SEM), Proximate and particle size analysis.

The rheological properties of oil well cement slurries (without FA), including viscosity and shear rate were investigated at three different temperatures in the range of 23 °C to 60 °C to determine the required lignosulphonate-based mid-range water-reducing admixture (LSM) to be used. This was done by means of an advanced shear-stress/shear strain controlled rheometer. The admixture LSM had a significant effect on the rheological properties of OWC by providing the necessary required chemical properties.

Furthermore, the OWC slurries with varying FA, in the range 0-30 mass %, distilled water and varying amount of LSM were cast and cured initially at room temperature for 24 hours followed by curing at $\pm$85°C for 2 days, 7 days and 28 days. The results obtained revealed that, the slurries mixed with a maximum of 30 percent amount of FA had a longer setting time as opposed to slurries without FA. The comparative study further indicates that, the longer the slurries were cured at higher temperature the higher the compressive strength. However, certain samples were reported to have a significant diminishing compressive strength and require further investigation in the future.

CHAPTER 1: INTRODUCTION

1.1 Introduction

The importance of crude oil in today's competitive business environment cannot be ignored due to the significant role it continues to play in the production of oil within the energy sector. The bulk of crude oil is used to produce fuels that are required for transportation, for instance, jet fuel, gasoline, and diesel. The production of oil begins with the creation of a crude oil well by drilling a hole into the earth with an oil rig. An oil or gas well can be thousands of meters in depth and not more than a meter in diameter (Nelson & Guillot, 1990). As such, this exercise is deemed to be quite costly. Hence, tremendous efforts have gone into inventions of equipment (including mud pump, top drive, fixed platform, Mobile jack-up rigs, etc…) that will drill wells at a cost-effective price (Drexler & Morgan, 1933). Drilling alone represents a large proportion of the total well cost (Young, et al., 1984).

Numerous reservoirs do not have adequate permeability to be deemed commercial unless the hydraulic fracture is created to connect more of the reservoir to the wellbore (Soliman, et al., 1988) In addition, cementing is one of the most critical steps in the drilling and completion of oil or gas wells. If not properly designed, the cementing operation may compromise the quality of the oil being drilled. Well cementing technology is the application of many scientific and engineering disciplines. It is for this very reason that it becomes imperative to select the appropriate type of cement due to the fact that typical Portland cement physical and chemical behaviour changes significantly when subjected to high temperatures and pressures (Souza, et al., 2012).

Table 0.1 The chemical composition of OWC and Portland Cement (Abuhaikal, 2016; Sancak et al., 2008).

	Abuhaikal, 2016; Sancak, et al., 2008		API specification 10A
	Class G Oil well cement (mass %)	Portland cement (mass%)	Class G Oil well cement (mass %)
C_3S	57	52	48 – 65
C_2S	17.3	19.6	20
C_3A	2.5	8.0	3 max
C_4AF	12	9.2	14.6
$C_4AF + 2C_3A$	17	25.2	24 max

Table 0.2. Physical and performance requirements (Abuhaikal, 2016; Sancak et al., 2008).

Class G Oil Well Cement as per API Specifications 10A	
Free-fluid content	5.9 % max
Minimum compressive strength	300 PSI (2.1MPa)
Setting Time	90 – 120 min

Oil well cement differs from Portland cement which is used for housing construction and concrete for construction work. The critical steps that it plays in drilling make oil well cementing arguably the most important operation performed on a well. Since well cementing technology is an amalgamation of numerous interdependent scientific and engineering disciplines which are critical to achieving the primary goal of well cementing, it must fulfil several functions. Among these are zonal isolation, oil and gas casing support, protection from any corrosive fluid formation, and the ability to withstand harsh conditions found underground (Thomas, 2005). Oil well-cementing systems are designed for temperatures ranging from below freezing in permafrost zones to 350 ^{0}C (662 ^{0}F) in thermal recovery and geothermal wells. They are also subjected to pressures ranging from ambient to 200 MPa (30 000 psi) in deep wells (Broni-Bediako et al., 2016).

Supplementing cement with FA in the casing for drilling purposes will be cost effective and will contribute toward revalorization of waste. Previous research by Daramola et al., 2017, looked at the beneficiation of South African coal fly ash in oil well-cementing operations at ambient temperatures, and the bottom-hole circulating temperature (BHCT) conditions of 52 ^{0}C and pressure 34.47 MPa (5000 psi). Salim and Amani (2012) paid special consideration in cementing high-pressure high-temperature wells, Shahriar (2011) investigated the rheology of oil well cement slurry. This research project has investigated the effect of particle size of fly ash and fly ash proportion on cement properties for drilling purposes in relation to high temperature and high pressure.

1.2 Research Question

The questions that were posed when carrying out this research are as follows:

1. What is the ideal particle type (Dura-Pozz /Super-Pozz) or size and amount of coal fly ash (FA) substitution in oil well cement (OWC) that can enable the cement to withstand the typical HPHT that is experienced during offshore drilling operations?

2. How well will the ideal compressive strength obtained from the cured slurry of OWC mixed with FA perform as compared to ordinary OWC slurry under HPHT?

1.3 Aim and Objectives

The aim of this research project was to assess and test the effect of particle type/size of coal fly ash (FA) on OWC properties for drilling purposes. The objectives of this research were as follows:

I. To evaluate the effect of temperature on OWC slurries mixed with different particle sizes of FA.
II. To measure the strength of oil well cement mixed with FA after being exposed to high temperatures.
III. To investigate the impact of LSM on the Rheological properties of a cement sample locally supplied by Pretoria Portland Cement (PPC) with similar chemical composition to class oil well cement (viscosity and shear rate).
IV. To investigate the impact of the various particle sizes of FA on the setting time and flow time of OWC slurries and the cement stability in various environments (offshore/ onshore).

1.4 Research Benefit

South Africa produces at least 32% of the total energy on the African continent. Eskom, being one of the largest energy utilities in the world produces approximately 95% of electricity consumed by South Africans and at least 45% of Africa's electricity. Eskom, primarily dependent on coal-fired power stations for electricity production is responsible for about 25 million tons of FA that are generated annually. This figure is set to increase when the new Medupi and Kusile power stations, which are still under construction are completed (Pretorius, et al., 2015). This statement and the recent discovery of gas condensate off the southern coast of South Africa by the petroleum company Total pave the way for the beneficiation of South African coal FA in the petroleum, oil and gas industry. Furthermore, the significance of this research is vested in the application of FA to produce a material that will cope with the harsh conditions of higher temperature and higher pressure that are consistent with offshore drilling operations. This research will add value to previous research that has already been conducted in the field of oil and gas engineering. Its exploration of the influence of different particle sizes of FA on cement properties and mortar strength will expand on areas that have been taken into consideration by previous research on FA used for drilling purposes.

1.5 Organisation of Research Report

This research report has been prepared according to the guidelines specified by the School of Chemical and Metallurgical Engineering. It has been divided into five chapters, including this chapter.

Chapter 1 is the introductory chapter which presents a brief overview of the importance of the petroleum industry and how the application OWC fits within the industry.

Chapter 2 reviews the literature of OWC. This includes the basic concepts involved in oil well cementing, the chemical and physical properties of oil well cement and a discussion on the role of related additives and chemical admixtures.

Chapter3 sets out a detailed description of the material and the methodology used in this research. The purpose is to provide information on the evaluation of the effect of temperature on OWC and measure the performance of OWC mixed with FA after being exposed to high temperature.

Chapter 4 discusses the results obtained from the research.

Chapter 5 provides the general conclusions drawn from this research and recommendations for future investigation.

CHAPTER 2: LITERATURE REVIEW

2.1 Introduction

The procedure of introducing cement slurry in the annulus between the casing and the geological formation is known as oil well cementing. Inadequate oil and gas well design and well cementing can jeopardise oil production. Cement by design is put in place to protect the outside of the well pipe and is used to seal off a well. Oil spills such as the recent Gulf of Mexico Deepwater Horizon incident are some of the catastrophic examples of the impact of inadequate oil well cementing (Shahriar, 2011). The successful drilling of an oil or gas well and the drilling fluid cannot fully prevent the well from collapsing. Therefore, it became vital in 1920 to introduce oil well cementing with clear objectives (Shahriar, 2011).

2.2 Basic cement compounds

There are four primary mineral compounds that makeup approximately 90 percent of Portland cement by mass. These compounds are tricalcium silicate (C_3S), dicalcium silicate (C_2S), tricalcium aluminate (C_3A), and tetra calcium aluminoferrite (C_4AF). C_3S is also known as alite and C_2S is also known as belite. The remaining portion of the cement consists of a calcium sulfate source, magnesium oxide, sulfur trioxide and grinding aids which are added during the grinding process. The calcium sulfate source, which constitutes two to five per cent as per South African Cement Specification, may be in the form of anhydrous calcium sulfate, calcium sulfate dihydrate, calcium sulfate hemihydrate, or a combination of these forms. Calcium sulfate dihydrate, also known as gypsum, is the most common source of sulfate in Portland cement. Hemihydrate is formed during the finish grinding of the cement (Kosmatka & Wilson, 2011).

2.3 Basic cementing process

The cementing of a well is a delicate and complex process, and well cement constitutes an essential barrier in the borehole that can be challenging to achieve. Since the production rate of wells is in decline due to the maturity of easy hydrocarbon fields, it becomes imperative to discover new wells. New discoveries are emerging primarily in areas representing complex challenges like depleted reservoirs, High-Pressure High-Temperature (HPHT) fields, unconventional source rock and fields in ultra-deep water (Løhre, 2015). It is for this reason that proper care should be taken into consideration from the onset to avoid offshore or onshore leaks. OWC may be pumped to depths over 6000m (20 000 ft) and at this depth, the

temperature may rise up to 205°C (400°F).

However, this temperature is usually reduced by the circulation of cooler drilling mud (Orchard, 1962, cited in Shahriar, 2011). The cement slurry may be subjected to very high pressures exceeding 200 MPa (30000 psi) depending on the height and density of the column of material above it (Joshi and Lohita, 1997, cited in Shahriar, 2011). Hence, oil and gas well cementing operations are subjected to additional challenges as opposed to common cementing work done above ground. Contamination emanating from the formation may also be of great concern as it may pose additional challenges. Consequently, OWC slurries are pumped between the well bore and the steel casing embedded in the well to seal off all strata of the formation, except those that have oil so that gases and water do not contaminate the oil bearing strata (Joshi and Lohita, 1997, cited in Shahriar, 2011).

The Deepwater Horizon disaster and the entire chain of events leading up to it should serve as a constant reminder to engineers in the oil well drilling sector to put measures in place that will foresee the improvement of cementing for drilling purposes (Mc Beath, 2016). Once a well has been drilled, the drill string is removed and a casing string which is accessorized with a float collar, guide shoe and centralizers is lowered into the hole until the shoe is almost at the bottom. The cementing head, containing the top and bottom cement plugs, is attached to the upper part of the casing string. The two plug system allows passage of the cement slurry through the casing whilst reducing the contamination of the cement slurry by drilling fluids that might have remained inside the casing before the pumping of the cement slurry commenced (Nelson & Guillot, 1990).

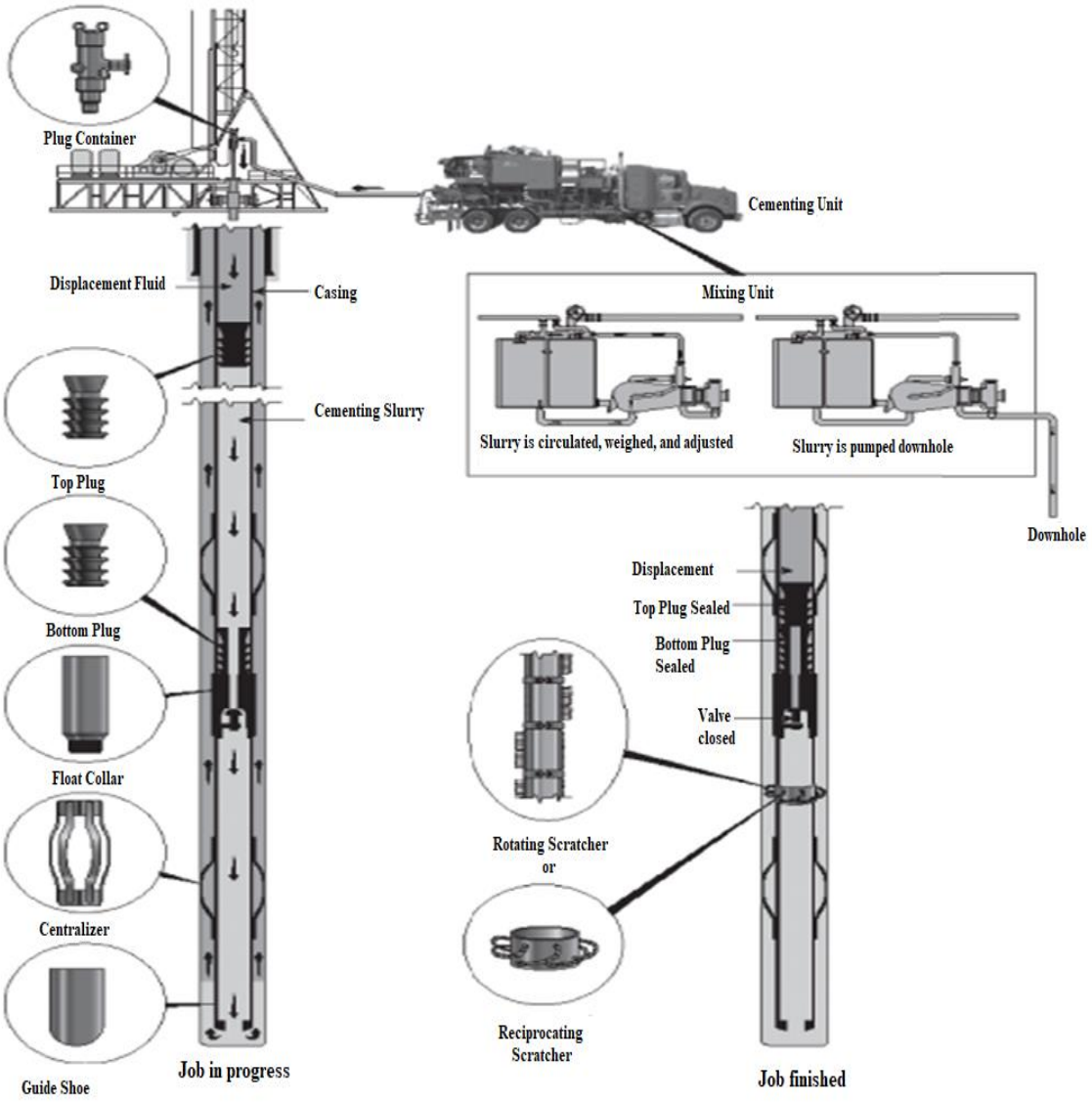

Figure 0.1 Cementing process (API, 2009; Nelson & Guillot, 1990).

2.4 The Basic Cementing Process for Drilling Purposes

The basic cementing process for primary cementing job makes use of two methods for pumping and displacement. Once the well has been drilled to the desired depth, the drill pipe will be removed to make way for a large string of casing that will run to the bottom of the well. The mud that was used to remove formation cutting must be cleared from the wellbore for cementing to be placed correctly (Nelson, 1990).

Primary cementing of oil or gas wells involves an adequate displacement of drilling mud by a spacer fluid and cement slurry. Several parameters, such as casing diameter relative to hole diameter, rheology of mud and cement, annulus eccentricity and flow rates of gas, must be taken into consideration. The goal of primary cementing is to provide support and protection

against the plastic formation and to seal off certain zones in order to prevent corrosive gases such as CO_2 or H_2S from reacting with cement. In the event where primary cementing fails, secondary cementing should be taken into consideration to seal off the required zones (Nelson & Guillot, 1990).

2.5 Oil Well Cements

Oil-well cements play a significant role in exploration and the production of oil and gas with additional applications in waste disposal, geothermal wells and sealing water wells (Ghabezloo, 2001). The American Petroleum Institute (API) Standard (API 10A: Specification for cements and materials for well cementing) categorises eight classes of oil well cements (OWC) for use at different well depths and conditions. OWC are specified in classes A–H and different grades corresponding to ordinary (O), medium sulfate-resistant (MSR) and high sulfate-resistant (HSR) (Nelson & Guillot, 1990). These classes of OWC have different requirements in physical properties and chemical composition (Ghabezloo, 2001).

The quality of cementing found between the well casing and surrounding strata may significantly affect the productivity of an oil well. A successful oil well cementing operation requires cement slurry to have flowability and stability. The properties of OWC slurries depend on the mix design and its components' quality. With cement being the most active component of the slurry, and the most costly, its selection plays an important role in obtaining the desired results (Shahriar, 2011). The common cement application may rely on type I or type II ordinary Portland cements for adequate strength and durability. However, oil wells may require other specific cement types in order to meet requirements that are consistent with HPHT.

The classes G and H are among OWC types reported to be the most widely used in terms of OWC, with the HSR class G requirements for C_3S mass set at a fraction between 0.48 and 0.65. C_3A fraction is smaller than 0.03 while C_4AF fraction smaller than 0.24. (Ghabezloo, 2001).

Table 0.1 Compositions of different class G OWC mass % (Ghabezloo, 2001).

	C_3S mass	**C_2S mass**	**C_3A mass**	**C_4AF mass**
G1	0.63	0.14	0.02	0.13
G2	0.51	0.27	0.02	0.14
G3	0.61	0.15	0.01	0.16
G4	0.59	0.15	0.02	0.19
G5	0.60	0.17	0.04	0.16

2.6 Admixtures for Well Cement

Oil well cementing has a minimal level of error tolerance in comparison to conventional cementing work (Shahriar, 2011). Consequently, the OWC slurry must be designed carefully to meet the demanding requirements that guarantee an overall durability. The ability to predict thickening time (set time), fluid loss control, consistency, low free fluid, low viscosity, high sulfate resistance and adequate strength is amongst the requirements of OWC.

In order to be pumped to greater depth, OWC slurries must have a particularly low viscosity. The down-hole HPHT compel stringent requirements on the setting behaviour of OWCs. OWC slurries usually incorporate Class G or H or other adequate cements, water, and chemical admixtures (Shahriar, 2011). Chemical admixtures play a significant role in regulating the early-age physical and chemical properties of cement slurries, and subsequently those of the hardened cementitious system. However, admixtures are known to have various shortcomings including variation of the initial slump, rapid loss of fluidity of cement slurries, and binder–admixture compatibility problems (Nehdi, 2012).

2.6.1 Types of Admixtures Used in OWC Slurries

Admixtures used in OWC slurries can be characterised into eight groups: extenders, set retarders, set accelerators, fluid-loss control agents, lost circulation control agents, weighting agents, dispersants and other specialty additives (antifoam agents, fibres, etc.) (Shahriar, 2011). The OWC slurry may incorporate extenders to lower the density of the cement system and increase its yield stress. Accelerators and retarders may be included to control the setting behaviour and weighting agents increase the density of the OWC slurry system. Different admixtures may also be used as dispersants or viscosifiers for the sole purpose of controlling the viscosity of slurry (Shahriar, 2011). In addition to mineral additives, supplementary cementitious materials (SCM) such as fly ash, powdered coal, rice husk ash, gilsonate, metakaolin, silica fume etc, may be used to modify certain properties of OWC (Nmegbu, et al., 2019).

2.7 Coal Fly ash (FA) and its use in cementing

2.7.1 Selection of Coal Fly Ash (FA) based on Classification and Benefits

FA in its primary nature is a by-product of burning pulverized coal in an electrical generating station and is recognized as an environmental pollutant (Ayanda et al., 2012). FA and bottom

ash are the two main types of coal residue obtained as by-products in the process of coal-fired electric power generation (Yazici, 2008). These tiny-sized earth elements are mainly made of silica, iron and alumina. When mixed with water and lime, the FA forms a cementitious compound with properties very similar to that of Portland cement (Stoch, 2015). Researchers have reported the usage of fly ash in concrete with cement replacement exceeding 30 %. In general practice, 30% FA replacement of cement in concrete is deemed suitable for durable concrete (Zulu & Allopi, 2016).

The usage of FA as a cement extender provides an immediate benefit for the environment as it will contribute immensely to waste reduction (Zulu & Allopi, 2016). Its applications in the construction industry reduce environmental and technical challenges with plants and decrease costs associated with electric power generation apart from reducing the amount of solid waste, greenhouse gas emissions associated with Portland clinker production, and conserve existing natural resources. Another aspect is that, each tonne of fly ash used in cement, or blended into the concrete mix, saves roughly one tonne of CO_2 emitted during the production of Portland cement (Zulu & Allopi, 2016).

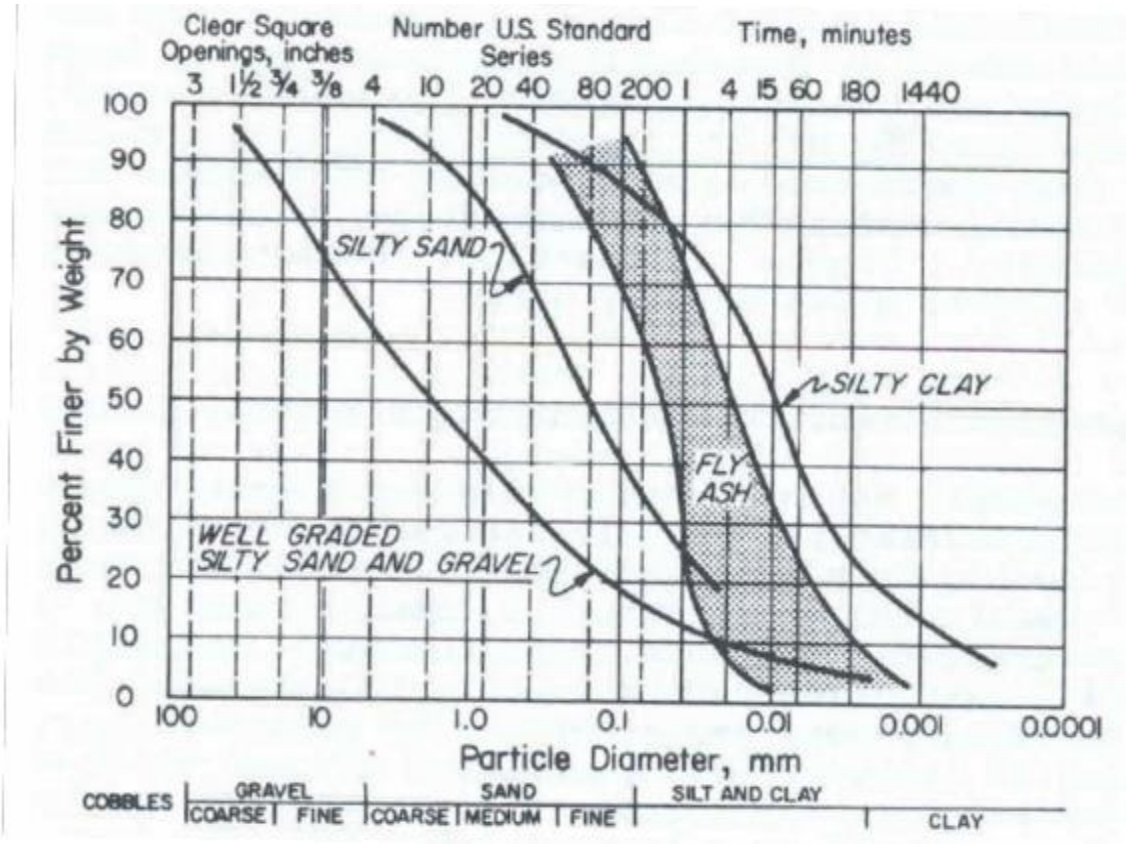

Figure 0.2 FA particle size compared with fine aggregate materials (Upadhyay & Kamal, 2007).

2.7.2 The Production of Coal Fly Ash (FA)

The production of FA requires burning off most of the coal volatile matter and combustion of the carbon in the furnace. This process traps the mineral impurities in the flue gas and blends them together. As the flue gas leaves the furnace, the ash is cooled rapidly and either agglomerates to form bottom ash or remains in the gas stream as FA. Before leaving the plant, FA is removed from the gases by electrostatic precipitators or bag filters. The material is comprised of spherical, glassy particles that generally may require no processing before it is used in concrete applications (Snellings, et al., 2012)

Although the use of FA in civil engineering and other construction applications is expected to rise, it is unlikely that this will ever get rid of all the ash being produced. Thus, ongoing research in line with alternative applications that can further exploit FA should be promoted. FA needs to be increasingly regarded as a raw material with potential for processing into new products rather than waste (Ilic, et al., 2003).

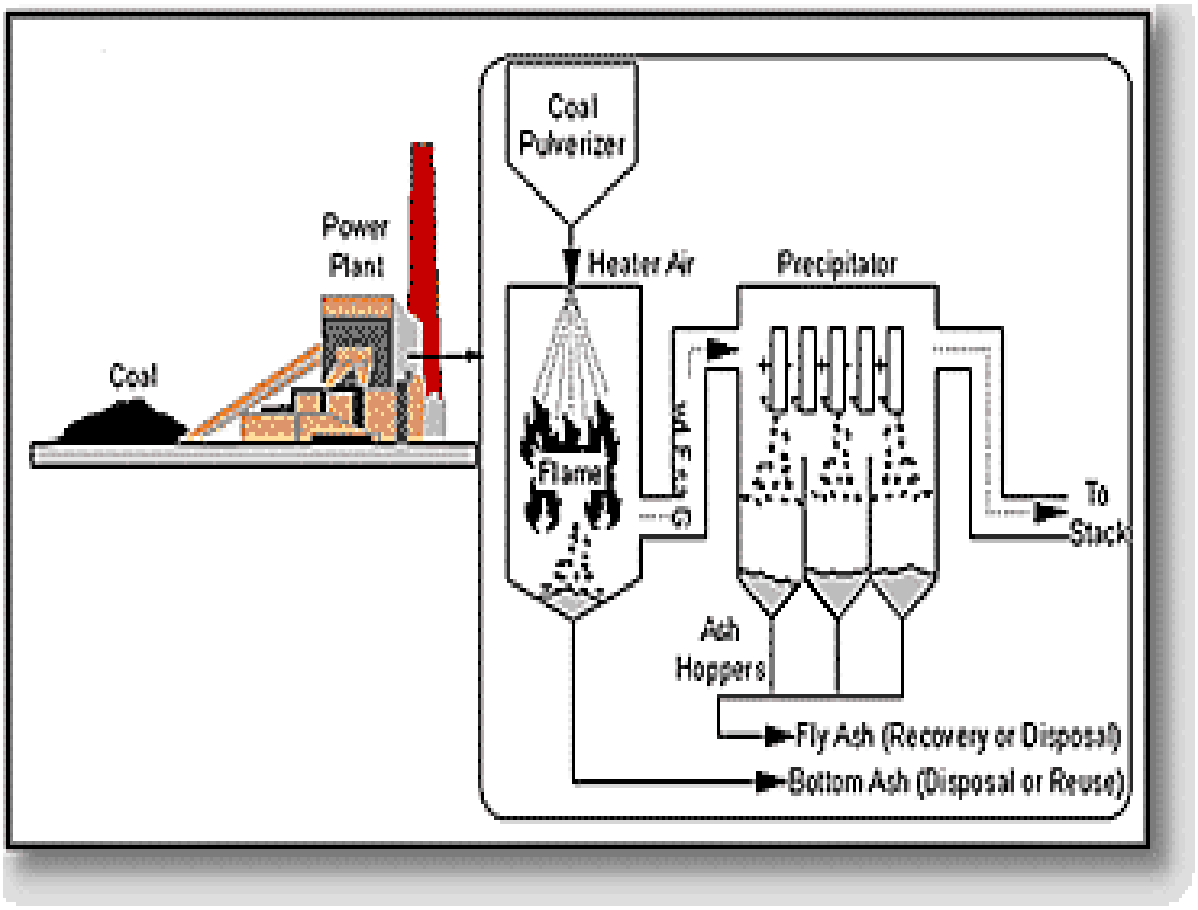

Figure 0.3 Production of FA in a dry-bottom utility boiler with an electrostatic precipitator (FHWA, 2016).

2.7.3 Coal Fly Ash Characterization

Fly ashes are generally categorized as low-calcium or high-calcium, which is in line with the American Society for Testing and Materials (ASTM) classifications of Class C and Class F, respectively (Obla, et al., 2003). Although the composition of fly ash may vary, the four major components that are present in most fly ash are iron oxide (Fe_2O_3), silicon dioxide (SiO_2), calcium oxide (CaO) and aluminium oxide (Al_2O_3). The source of coal used during production is a determining factor of the composition found in fly ash (Obla et al., 2003). Four types of coal are known to be in existence and these may vary in ash content, chemical composition, heating value and geological origin. The four types of coal are sub-bituminous, anthracite, lignite and bituminous. In addition, FA can be handled in a wet, dry or conditioned form (Ahmaruzzaman, 2010).

The main components of bituminous coal FA are iron oxide, silica, alumina and calcium oxide with different amounts of carbon as quantified by the loss on ignition (LOI). Sub-bituminous and lignite coal FA ash are characterized by reduced percentages of iron oxide and silica, higher concentrations of calcium and magnesium oxide and lower carbon content when compared to bituminous coal fly ash (Ahmaruzzaman, 2010). Anthracite coal FA is found only in a small amount due to little quantity being burned in utility boilers. Table 4 shows the normal range of chemical composition for fly ash produced from different coal. From the table, it is evident that both sub-bituminous coal and lignite FA have a higher calcium oxide content and lower Loss on ignition when compared to FA from bituminous coals. Sub-bituminous and Lignite coal FA may include a higher concentration of sulfate compounds than bituminous coal FA (Ahmaruzzaman, 2010).

According to the American Society for Testing and Materials (ASTM), the sum of the Fe_2O_3, SiO_2, and Al_2O_3, constituents of a FA must be greater than 70% to be classified as Class F (Obla et al., 2003), while ASTM C618 (2013) makes provision for those with a (Fe_2O_3+ SiO_2+Al_2O_3) content ranging between 50 and 70 wt% and high in lime to be defined as class C. In essence, the high-calcium Class C FA is normally produced from the burning of low-rank coals (sub-bituminous or lignite coals) and it comprises cementitious properties when reacted with water (Ahmaruzzaman, 2010). However, this sum is lower than what is required for Class F, since most Class C fly ashes have CaO contents exceeding 20% (Obla et al., 2003).

This allows for much lower CaO concentrations than in Class C FA. Because of this, Class F fly ashes normally have very little or no cementitious properties of their own and are primarily

Pozzolanic (Obla et al., 2003). Another difference that sets Class C apart from Class F is the amount of alkalis (combined sodium and potassium), and sulfates (SO_4), are generally higher in Class C FA as opposed to Class F FA. In the South African National Standard on FA (SANS 50450-1:2014) as adopted from EN 450-1:2012, the European standard for FA content as an extender, the usage of FA is allowed up to 55 percent level of clinker replacement (Du Toit, et al., 2015). However, it should be noted that SANS 50197-1 for cement allows up to 35% FA for a CEM II Portland FA cement, and up to 55% for a CEM IV Pozzolanic cement.

Table 0.2 The normal range of chemical composition for FA produced from different coal (Ahmaruzzaman, 2010).

Composition (wt. %)	**Bituminous**	**Sub-bituminous**	**Lignite**
SiO_2	20-60	40-60	15-45
Al_2O_3	5-35	20-30	10-25
Fe_2O_3	10-40	4-10	4-15
CaO	1-12	5-30	15-40
MgO	0-5	1-6	3-10
SO_3	0-4	0-2	0-10
Na_2O	0-4	0-2	0-6
K_2O	0-3	0-4	0-4
LOI	0-15	0-3	0-5

Table 0.3 . Difference between class F and class C FA; class N and S fly ash (SANS 50450) (ASTM C618) (Sutter, 2013) (50450-1, 2014)**.**

		ASTM C618		**SANS 50450**	
		Class F	**Class C**	**Class N**	**Class S**
Chemical: $SiO_2+Al_2O_3+Fe_2O_3$	%	>70	>50	>70	>70
Physical: + 45 µm	%			<40	<12

2.8 Effect of Fly Ash on Hydration

The hydration of the calcium silicates in Portland cement produces calcium silicate hydrate (C-S-H) and calcium hydroxide (CH) (using the cement industry notation). Beside a Pozzolan such

as FA, silica is added to the mixture and this will react with CH in the presence of water to form C-S-H. This is known as the Pozzolanic reaction. The Pozzolanic reaction is relatively slow and results in slower rates of heat evolution and strength gain. However, the consumption of CH and filling of pores in the paste will act as a beneficial factor that will lead to higher ultimate strengths and improved durability (Mindess & Darwin, 2003).

Jiang et al. (1999) studied the hydration of paste mixtures made with Portland cement and Class F fly ash at 40, 55, and 70 per cent replacement levels. The process entailed varying the w/c ratio and included water-reduction and activating admixtures in some of the pastes. It was discovered that, when compared to the control mixture, FA mixtures had lower early strengths but improved in strength later as the days of ageing progressed. The CH content of the mixtures, in general, will decrease after 28 days. From pore structure analysis, it was determined that the total porosity at 28 days increased with increasing fly ash content. However, the pore size distribution showed that the pore sizes were decreased with the inclusion of fly ash.

2.9 Effect of Fly Ash Volume on Paste Properties

2.9.1 Compressive Strength

A Pozzolanic reaction is known to be slow. This, in turn, will determine the rate at which a class C fly ash and cement mixture will gain strength. However, the pozzolanic reaction will yield greater strength as the cement paste matures. This is due to the replacement of the weak CH products with C-S-H, which is stronger, and by filling pores with pozzolanic reaction products. This reduces the overall porosity of the paste and leads to an increase in strength (Detwiler & Mehta, 1989).

Research conducted by Bentz, et al. (2010) evaluated the strength gain characteristics of mortars containing 50 percent of either Class C or Class F fly ash. The strengths were assessed at 1, 7, 28, 56, 182, and 365 days respectively. The findings were such that, one-day strengths of the fly ash mixtures were roughly only 30 percent of those achieved with the 100 percent cement mortar. At later ages, it was reported that the strengths of the mixtures were close to that of the control specimen. Once the specimen had reached 365 days, the evidence revealed that all of the mixtures with 50 per cent FA had compressive strengths that were greater than 85 per cent of the strength of the control mixture (Bentz, 2010).

2.9.2 Setting Time of OWC Slurries

As explained above, OWC is exposed to a wide range of pressure and temperature, which has implications on the time required for setting and hardening. Setting time commences as a result of development of a cross-linking structure of hydration products soon after the dormant period. Good control of setting time is achievable when C_3A reactivity is matched with soluble-sulfate availability (Alsop, 2014) .

2.9.3 The effects of Fly Ash on properties of OWC slurry

The mixture of cement with water triggers a reaction that eventually produces the binder that joins the slurry mass (Berry & Malhotra, 1986). New particles are formed, and original particles dissolve or are coated with cementitious products. The forces of dispersion, flocculation, and gravity compete to determine the spatial distribution of the materials in the changing mass. The spherical particle shapes of fly ashes are known to increase the followability of cementitious mixtures. This is due to the role that spherical shape plays in reducing friction between particles in the mixture (Mindess et al., 2003).

The temperature rises as a result of the chemical reaction that eventually release heat. In all these events, FA plays a significant role by making use of its low-calcium to act largely as a fine aggregate of spherical form. High –calcium FA on the other hand may participate in the early cementing reactions, in addition to being part of the particulate suspension (Berry & Malhotra, 1986). Since OWC slurries are mixed and placed, frequently in heavily reinforced formwork, it is necessary that in most cases a level of fluidity, generally called workability, be maintained. This is determined by the rheological properties of the system which are influenced by all of the components. Control of workability is one of the objectives of cement mix proportioning. Thus, it becomes imperative to understand the role of FA in the rheology of fresh slurries if the optimum exploitation of its properties is to be made (Berry & Malhotra, 1986).

2.10 Summary

In this chapter, research pertaining to oil well cementing has been reviewed along with previous studies conducted on additives, rheology of oil and well cements. It is noted that successful oil well cementing process must fulfil two basic criteria: the ability to be pumped easily and to allow sufficient time for proper placement of the slurry in the well bore subjected to HPHT. The cement slurry should also develop and maintain adequate mechanical strength

to protect and support the casing. It must have low permeability and adequate durability to ensure the long-term isolation of the producing formation. With the introduction of API OWC specifications. Achieving the above has been made easy. In addition, mineral additives and chemical admixtures play an important role in changing the physical and chemical properties of the oil/gas well cement slurry by maintaining the proper rheology necessary for the placement of the cement slurry in typically deep well bores.

CHAPTER 3: EXPERIMENTAL PROCEDURE AND ANALYTICAL PROCESS

This chapter covers the methodology used during this study. This investigation was divided into four stages:

i. Characterisation of FA and OWC by SEM, XRD, XRF, PSA, TGA
ii. Rheological tests of OWC with Additives at 25°C, 45°C, 60°C
iii. Setting Time
iv. Cement casting (Preparation of OWC slurries with various quantities of FA and LSM)
v. Compression test (cured OWC samples compressive strength and analysis of OWC slurries for density)

Figure 3.1 below, elaborate on the different procedures that were carried out in the study. Various samples using fly ashes (Dura-Pozz and Super-Pozz) and a cement sample locally supplied by Pretoria Portland Cement (PPC) with similar chemical composition to class oil well cement were used for the tests experiment. The characterisation of material was done by means of XRF, XRD, PSA, TGA and SEM. The particle size distribution was done to retain 45μm of fly ashes. The supplied PPC cement (45kg) was mixed with Lignosulphonate (LSM) (3.645kg) to test for rheology by means of an Anton Paar Rheometer and obtain cement with similar physical characteristic to class G oil well cement. Once the desired amount of LSM was obtained, various proportions of fly ashes were mixed with cement and slurries were cast. Setting times were done using a Toni SET compact – Automatic Vicat Needle instrument. Curing was done (16 hours, 2 days, 7 days and 28 days) followed by compressive strength determination using a ToniCom III compressive strength testing machine with a capacity of 1600 kN.

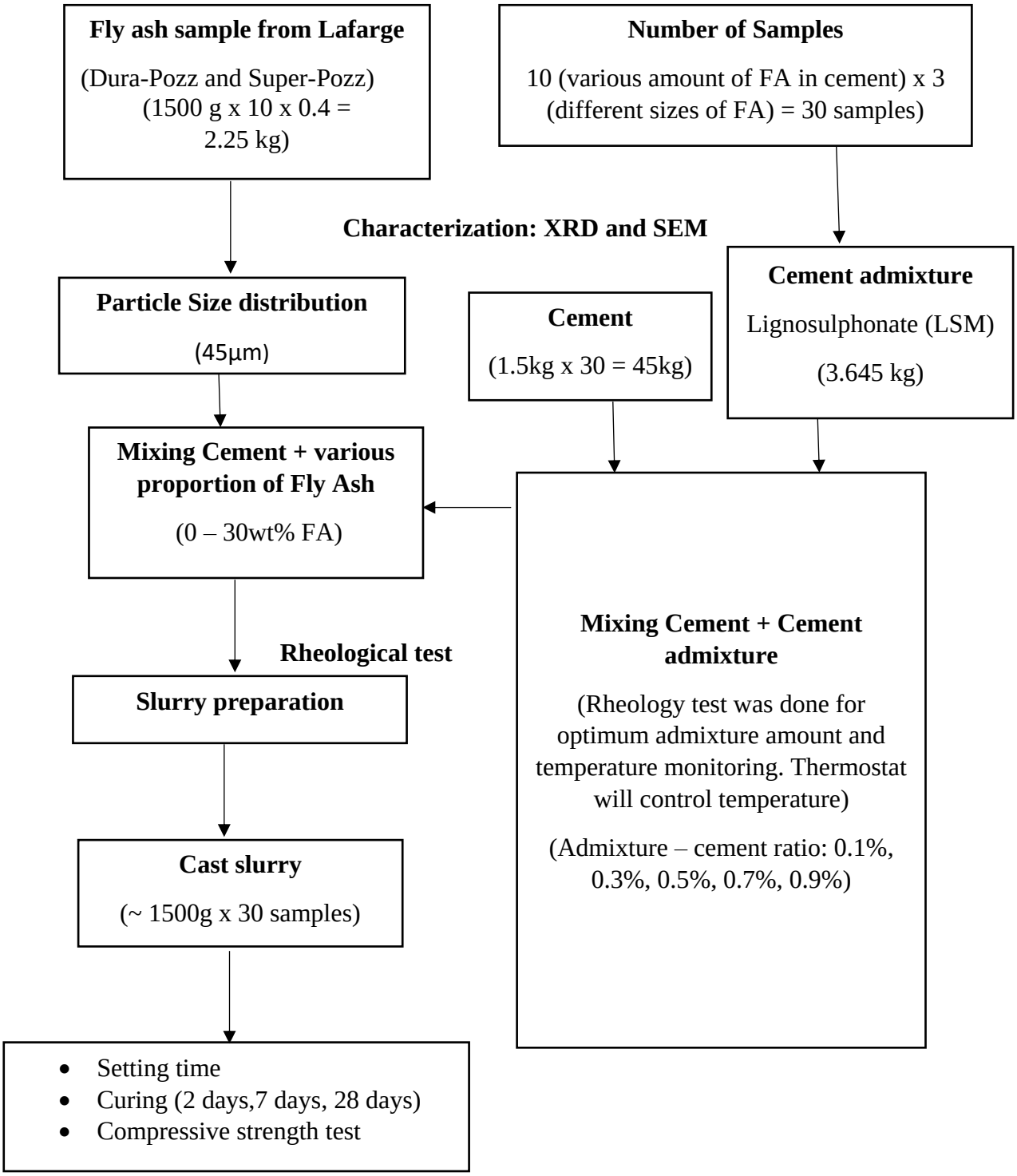

Figure 0.1 Flow Chart and sample details

The final test cement composition was achieved by means of an additive (LSM).

3.1 Cement and FA Sampling

The process of reducing a large quantity of material to a smaller portion which is a representative of the whole is of great importance, more especially with raw materials where large particle size and heterogeneity require that massive samples are taken and reduced systematically to the quantity actually analysed (Alsop, 2014). In this instance, the samples were brought into the laboratory 24 hours prior to the commencement of the experiment to acclimatise with the laboratory environment set at ± 23 ^{0}C. A hand size sample of cement with close characteristic of OWC class G was collected from the sample donated by PPC in South Africa. Small quantities of cement were randomly scooped from the homogenised PPC OWC. The same sampling process was repeated for the various FA samples obtained from Lethabo Power Station in the Free State Province, South Africa and Secunda in Mpumalanga Province, South Africa. This sampling method was used for both OWC and FA to ensure quick collection and sealing away of materials to minimise errors that may arise as a result of keeping samples open for a longer period (Wills & Napier-Munn, 2006). A detailed chemical and mineralogy analysis using X-ray Fluorescence (XRF), X-Ray Diffraction (XRD), Scanning Electron Microscopy (SEM), and particle size analysis for both cement and FA was conducted.

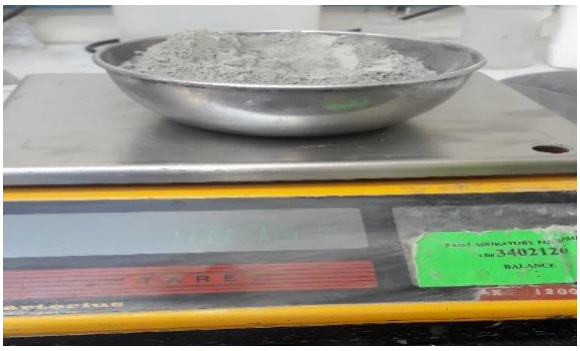

Figure 0.2 Weighing of cement

3.2 Characterisation techniques and Chemical analysis

3.2.1 X-ray fluorescence (XRF) background

EN 196-2.2 (methods of testing cement) was the first European standard for XRF analysis of hydraulic cements and is the basis of ISO 29581-2 Cement test methods-part 2: Chemical Analysis by X-Ray Fluorescence. A similar standard has been developed for the current edition of ASTM C114 which include precision and accuracy requirements for all methods. (Alsop,

2014). It should be noted that calibration is required prior to using XRF and other methods are in existence for analysis of materials such as cement or FA (Alsop, 2014).

3.2.2 Preparation of XRF bead

A1g portion from the ignited sample was weighed in a platinum crucible and 8g of the flux was added into the crucible with the sample then fused in a fusion machine for 18 minutes in the Nieka G4A automatic fusion machine as shown in Figure 3.3 to form a bead. The bead was then placed into an XRF spectrometer for oxides analysis.

In order to determine the elemental composition of the FA and cement, a Bruker S8 Tiger XRF spectrometer as shown in figure 3.3 was used for the analysis. Each sample was ground to 100% passing 45 microns (μm).

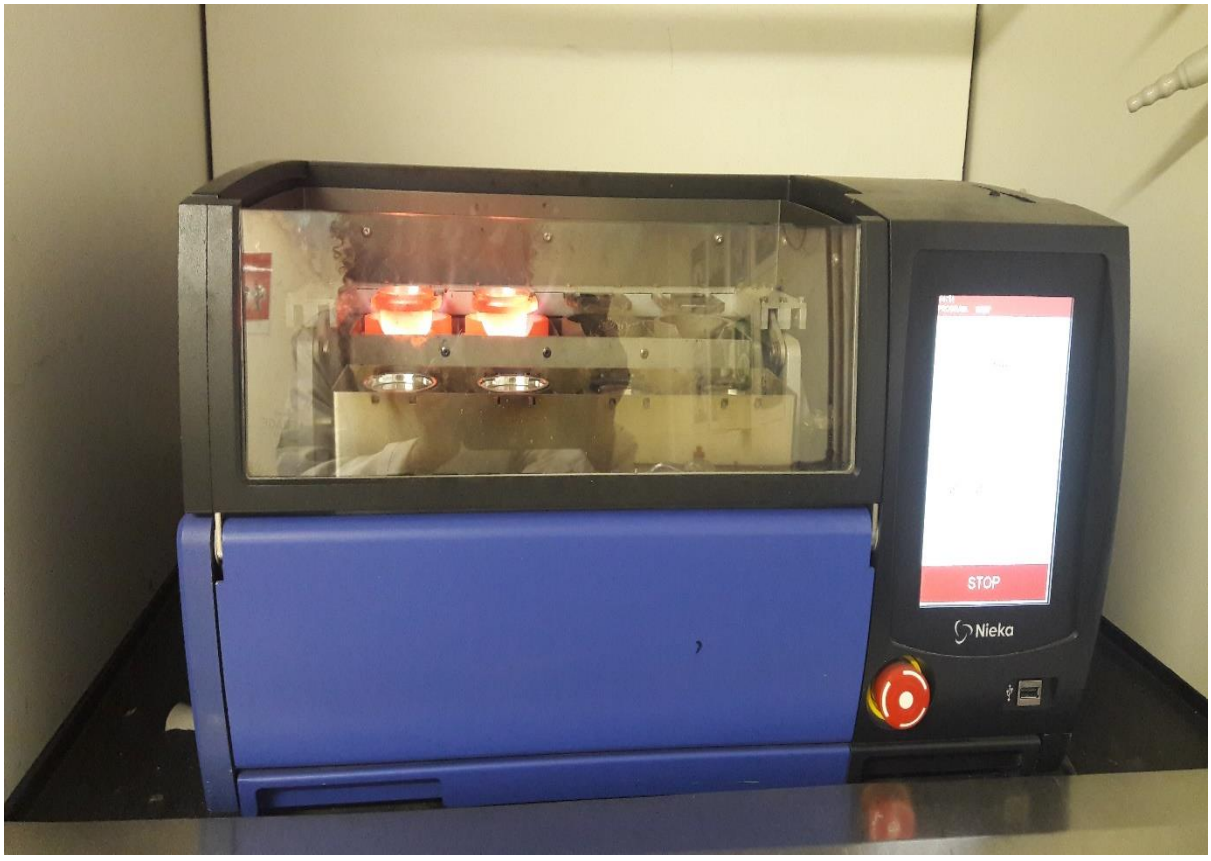

Figure 0.3 The Nieka G4 A automatic bead fusion machine

3.2.3 Loss on ignition (LOI)

Figure 0.4 The Bruker S8 Tiger XRF spectrometer

The purpose of LOI is to determine the residue of unburnt carbon in the FA. The LOI was determined in accordance with the EN 196 – 2 standard methods. The FA samples and OWC were used. Approximately 2 g of the sample was weighed on a balance in a crucible. It was then placed in a laboratory furnace (the Scientific furnace) at 950°C as shown in Figure 8 for an hour. After an hour, it was removed from the furnace, and placed in a desiccator to cool to room temperature. Samples were weighed after cooling and loss on ignition was obtained using the following formula:

$$\% \, \mathbf{LOI} = \frac{\mathbf{D}}{\mathbf{B}} * \mathbf{100} \, \%$$

A - Empty crucible (g); B - mass of sample (g); C - mass of crucible plus residue after heating;

D - Weight loss = A+B-C.

Figure 0.5 The Scientific laboratory furnace

3.2.4 X-ray diffraction (XRD)

X-ray powder diffraction (XRD) offers the ability to identify and quantify chemical compounds such as $CaCO_3, CaSO_4.\frac{1}{2}H_2O, CaSO_4.2H_2O$, quartz, free lime, free magnesia (periclase), clinker phases and other mineral phases in conventional and alternative raw materials. Most other techniques measure concentrations of elements and then report these as oxides (Alsop, 2014). A quantitative analysis of OWC and the various FA samples were done using a D2 PHASER Bruker X-ray diffractometer (XRD). Diffrac.EVA software was used for phase analysis of the XRD patterns.

Figure 0.6 X-ray diffractometer for powders - D2 PHASER – Bruker

3.2.5 Proximate Analysis

To carry out a proximate analysis on the OWC cement sample and FA samples, a combined Thermogravimetric Analysis (TGA) and; Differential Scanning Calorimetry (DSC), PerkinElmer STA 600 Simultaneous Thermal Analyser with Pyris software was used (Fina, et al., 2006). Thermogravimetry is a standard method used for analysis of inorganic, organic and synthetic materials. The purpose of TGA analysis in general, is to record the measurement of the weight loss during a user-defined temperature or heating process. The purpose was to determine moisture content, Loss on ignition (LOI) and amount of volatiles in the cement and FA. Initially, a crucible was tared to zero at 30 °C. A sample weighing approximately 10 mg was put in the crucible and gently lowered into the furnace using a pair of tongs. The sample weight was normalized and the proximate analysis program was run. When the program finished running, the crucible was removed from the furnace using a pair of tongs.

3.2.6 Scanning Electron Microscopy (SEM) Analysis

A representative portion of the OWC and FA samples was coated and put onto double-sided carbon tape mounted on a SEM stub. This grain mount allows for analysis of particles that determine the morphology of a specific sample, the external surface structure and external elemental distribution of individual FA particles or OWC (Kutchko & Kim, 2006). The morphologies of OWC and FA were analysed using a ZEISS Sigma VP Field Emission-Scanning Electron Microscope (SEM). The samples were initially sputtered with a double coat of gold and palladium, 10 μm thick. The sputter coating gives the samples the advantage of increased thermal conduction, reduction in microscope beam damage and reduced charging. The coated samples were then placed in the SEM instrument where a microscope scanned a focused electron beam over their surface and created images with varying magnifications.

3.2.7 Particle Size Analysis

A Malvern Mastersizer 2000 was used to determine the particle size distribution of the OWC and the FA samples. The samples were wetted by means of deionized water. The cement and the FA were dispersed in de-ionized water and an ultrasonic probe was used to ensure complete dispersion. Once full dispersion had been completed, the ultrasound probe was switched off and the particle size was monitored (Kaduku, et al., 2015).

Figure 0.7 Malvern Mastersizer 2000

3.3 pH Analysis

The purpose of pH analysis was to determine the acidity/basicity of the mixture of fly ashes and cement in water. The pH of cement and FA dissolved in water was measured using a Metrohm 744 pH meter. 100 g of cement sample and 100 g of various FA samples were separately added to 1000 ml de-ionized water at 25 °C. The slurry was stirred using a magnetic stirrer at 250 rev/min. The change in pH of the slurry was monitored at 1 minute intervals until it became constant.

3.4 Mixing and preparation of cement slurry for rheology test

The purpose of rheology is to determine the quality of the hardened cementitious matrix and assist in predicting its physical properties and end-use performance (Nehdi, 2012). For this determination, the cement slurries were prepared using a high-shear blender type mixer with bottom-driven blades as recommended (API, 1990). The procedure was as follows: at first, the weighed amount of cement as indicated in Table 3.1 was placed into a bowl for preconditioning at 150 rpm for a period of 10 minutes. The mixing water was kept constant at 50 ml. The water was then poured into the blender. The various required quantities of Lignosulphonate (LSM) (0.1%, 0.3%, 0.5%, 0.7%, and 0.9%) liquid admixture were added to the water using a syringe, and the mixing started at a slow speed for 10 seconds to allow the chemical admixtures to be thoroughly dispersed in the water. Manual mixing was conducted for 15 seconds and a rubber spatula was used to recover material sticking to the wall of the mixing container to ensure homogeneity.

Finally, mixing resumed for another 35 seconds at high speed. This mixing procedure was strictly followed for all cement slurries. All mixing was conducted at a controlled ambient temperature of 23 ± 1°C. The prepared slurries were then placed into the bowl of a mixer and stirred for over 10 min at a speed of 150 rpm.

A high accuracy advanced rheometer as indicated in Figure 3.9 was used for the duration of this study to measure the rheological properties of the cement slurries. The bottom hole circulating temperature (BHCT) used for this rheology test was 23 °C, 45 °C and 60 °C. The total time between the beginning of mixing and the start of the rheological tests was kept constant to avoid the effect of exogenous variables on the results. The rheometer set-up was also maintained constant for all prepared mixtures of slurries. The concentric cylinder test geometry was kept at the test temperature so as to avoid sudden thermal shock to the slurry.

The following parameters of the slurries were studied: shear thinning, plastic viscosity, Apparent viscosity and yield stress. The slurry cementitious compositions are shown in Table 3.1.

Table 0.1 Determination of admixture (LSM) dosage

Mass of Cement(g)	Admixture number of drops	Mass of Admixture (g)
109.89	5	0.1
102.36	14	0.3
105.07	24	0.5
102.99	33	0.7
106.59	44	0.9

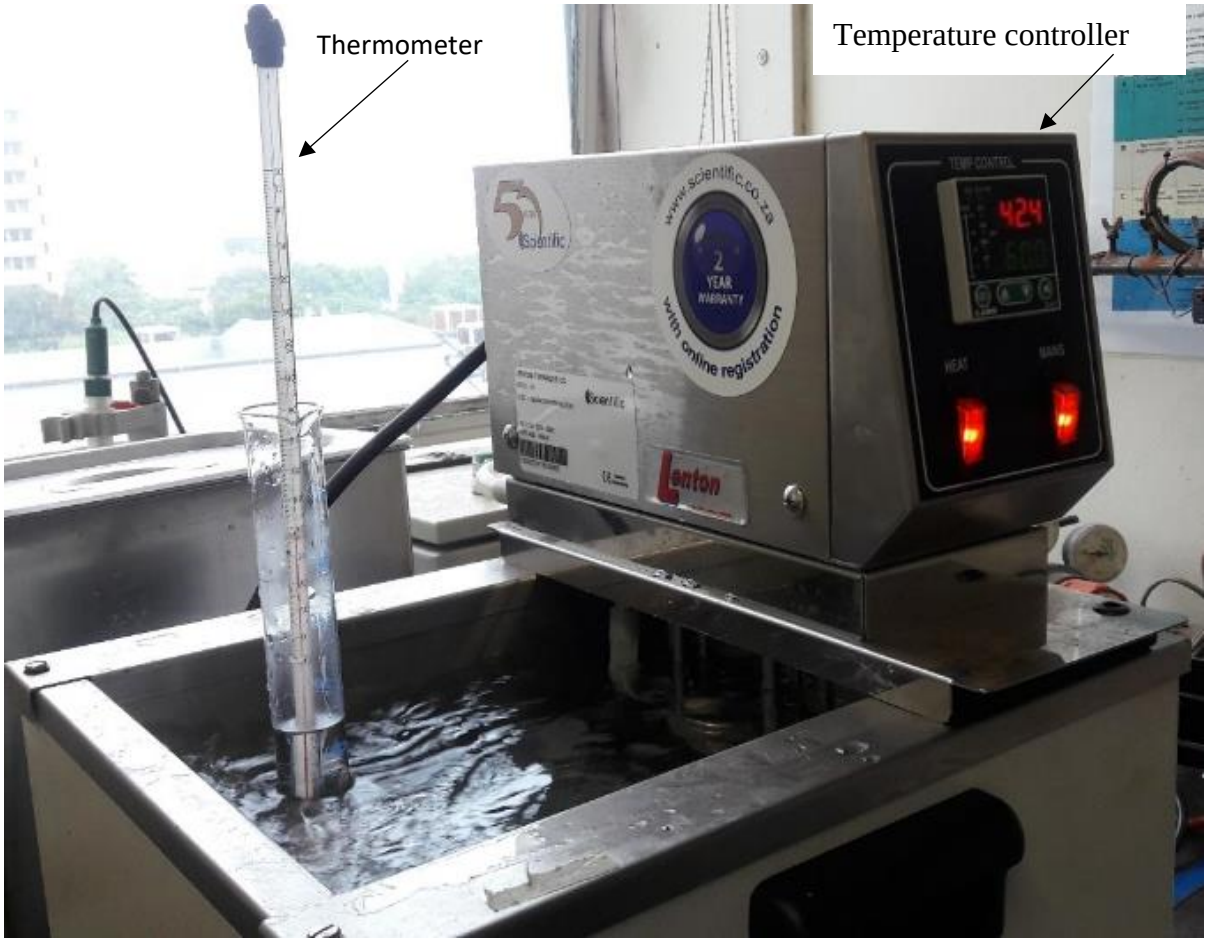

Figure 0.8 Water bath for Rheology test preparation

Figure 0.9 Anton Paar Rotational Rheometer: RheolabQC

3.5 Standard Consistency

The standard consistency test is performed using a Vicat plunger in order to determine the consistency at which the plunger penetrates to a point 4-8 mm from the bottom of Vicat mould in a freshly- prepared cement/water mix.

The standard consistency is determined as:

(Mass of water) / (Mass of cementitious material) expressed as percentage (%).

The Vicat setting test (ASTM C191) (SANS 50196-3), is the accepted method used to determine the initial and final setting times for hydrating cementitious mixtures as well as the standard consistency.

In determining setting times, - increasing structure formation acts to reduce the extent of penetration into the specimen. In this test, the initial and final sets were identified at penetration depths of 25 mm and 0.5 mm, respectively, for pastes having a normal consistency. At these penetration depths, the material has a shear resistance of ± 32 and 900 kPa, respectively (Zhang,

et al., 2010). In order to determine the standard consistency of the cementitious material, three test runs were performed as indicated in Table 3.2.

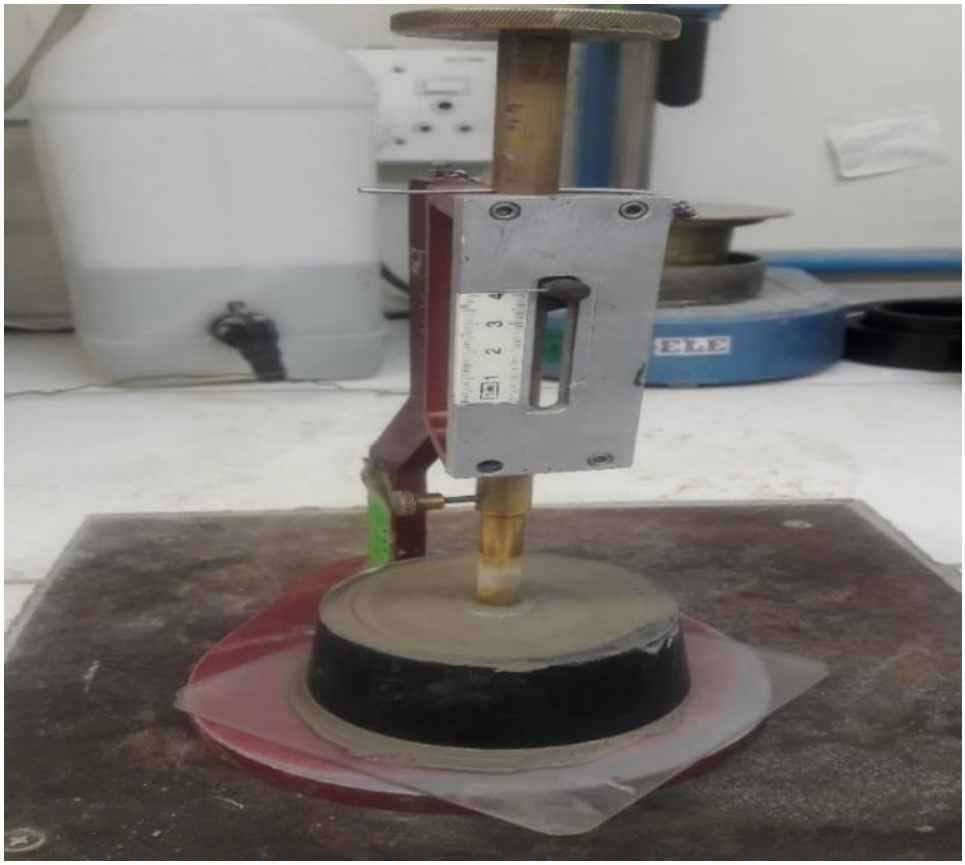

Figure 0.10 The Vicat plunger test for OWC

Table 0.2 Standard Consistency of OWC

Date	7/3/2019	Sample ID	OWC
Sample Description	OWC	Lab Temperature	25 °C
Balance ID	3402126	Mixer ID	HM157
Time ID (clock)	WC4	Vicat mould ID	H
Plunger ID	V0A009	Vicat ID	E
Reading of plunger on the glass plate	0	Water Temperature	23 °C
Lab Humidity	54.1%		
	Run 1	**Run 2**	**Run 3**
Mass of Water	134.3 g	134.3 g	134.3 g
Mass of Cement	500 g	500 g	500 g
Mass of Ash	0 g	0 g	0 g
Depth of Plunger	7 mm	7 mm	7 mm
Time water added	2:35 pm	2:45 pm	2:55 pm

Standard Consistency = Mass of water / Mass of cement *100 = 26.86%

3.6 Standard Consistency of cement and fly ash at varying ratios

The same process undertaken to determine the standard consistency of OWC was also undertaken for OWC and 30% FA mix. In order to determine the standard consistency of the cement and 30% FA mix, three test runs were performed as indicated in Table 3.3.

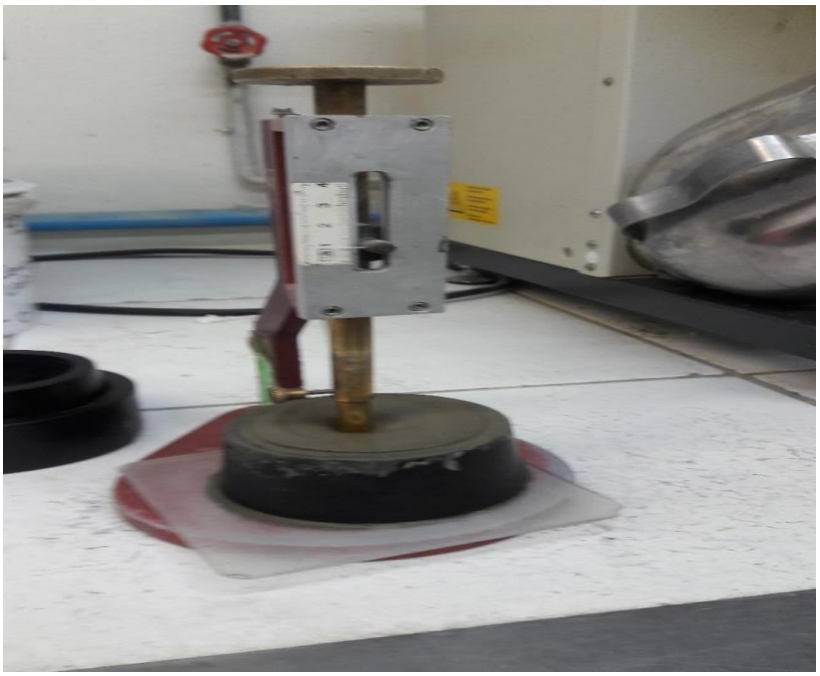

Figure 0.11 The Vicat plunger test for 30% FA standard consistency

Table 0.3 Standard Consistency of OWC Blended with FA

Date	7/3/2019	Sample ID	OWC
Sample Description	OWC blended	Lab Temperature	25.1 °C
Balance ID	3402126	Mixer ID	HM157
Time ID (clock)	WC4	Vicat mould ID	D
Plunger ID	V0A009	Vicat ID	E
Reading of plunger on the glass plate	0	Water Temperature	23 °C
Lab Humidity	54.6%		
	Run 1	**Run 2**	**Run 3**
Mass of Water	128.3 g	128.3 g	134.3 g
Mass of Cement	350 g	350 g	350 g
Mass of Ash	150 g	150 g	150 g
Depth of Plunger	6 mm	6 mm	6 mm
Time water added	3:51 pm	4:01 pm	4:11 pm

Standard Consistency = Mass of water / Mass of cement *100 = 25.66%

3.7 Setting time

Setting of cement is triggered by the development of a cross-linking structure of hydration products soon after the dormant period (Alsop, 2014). Good control of setting is achieved by matching C_3A reactivity with soluble-sulfate availability. An imbalance between C_3A reactivity and sulfate availability can cause flash set or false set (Alsop, 2014).

Knowing the setting time of OWC is of paramount importance for scheduling the oil well drilling operation. It is therefore advisable to have such information at hand. Once the cement is pumped into place, the well is left shut for a sufficient time to allow the cement to harden before resuming drilling to a greater depth (Zhang, et al., 2010).

In this instance, the cement paste to be tested were prepared as per Table 3.2 and Table 3.3 specifications. The OWC and FA/OWC pastes obtained from the Vicat plunger standard consistency test (as observed in Figure 3.10 and Figure 3.11) were placed with the cylindrical ring into the Toni SET Compact Automatic Vicat Needle Instrument. The computer was then set up to release the needle for penetration and step-wise measurement of the setting progress. The initial and final setting times of the cements pastes in accordance with SANS 50196-3 were recorded.

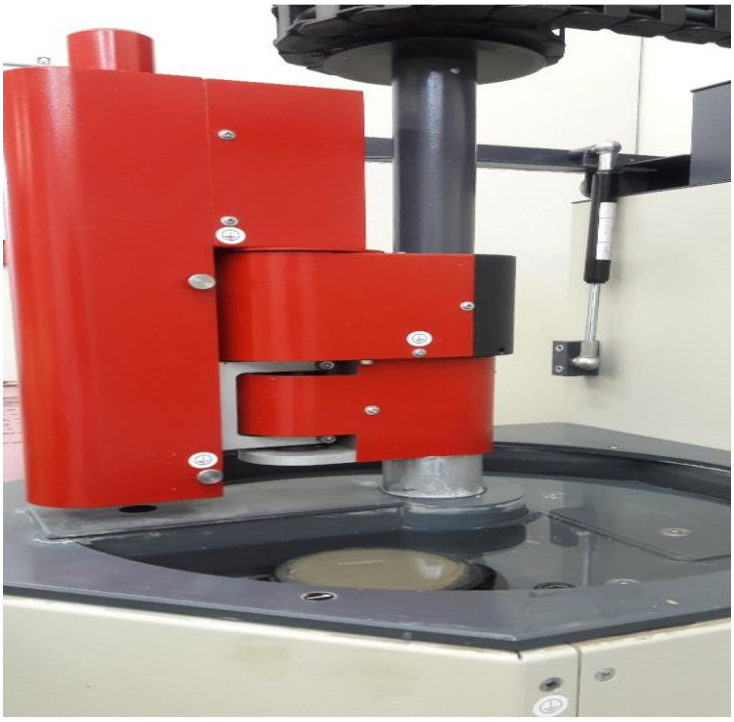

Figure 0.12 Toni SET Compact - Automatic Vicat Needle Instrument

3.8 Determination of soundness for OWC

The purpose of this experiment was to test for expansion and structural stability in a hot environment SANS (Akindahunsi & Uzoegbo, 2015). In order to perform this test, the cement pastes were mixed as per the standard consistency test specifications. The samples were cured for 24 hours before being placed in a water bath at a maximum temperature of 92 °C. The prepared cement samples were then immersed in the water bath as per Figure 3.14 and data was collected at per Table 4.1.

Figure 0.13 Soundness of OWC

3.9 Determination of soundness for cement mixed with FA

Checking of expansion – data was collected at per Table 3.4.

Figure 0.14 Soundness for OWC with FA

3.10 Mixing and preparation of cement slurry for casting purposes

The slurries with a constant amount of cement and Lignosulphonate based mid-range water-reducing admixture (LSM) as well as varying amounts of water and FA were prepared. The slurry compositions are shown in Table 3.4. Deionised water was used at room temperature (±23 ^{o}C). A Hobart mixer conforming to SANS 50196-1 was used to mix the slurry. A Hobart is a high-shear blender type mixer with top-driven blades in accordance with the specification for materials and testing for well cements (API, 1990); (Msinjili & Schmidt, 2015).

The cement was placed in a measuring cup and the required amount of LSM was added to the mixing water by means of a syringe. The mixing was started at a slow speed for 10 seconds to thoroughly disperse the chemical admixtures in the water. In order to ensure that there was no waste in terms of material, the liquids (liquid admixture and water) were added to the cement for a period of 10 seconds. Manual mixing was conducted for 15 seconds and a rubber spatula was used to recover material sticking to the wall of the mixing container to ensure homogeneity. Lastly, mixing continued for another 60 seconds at high speed. This mixing procedure was strictly followed for all cement slurries. All mixing was conducted at a controlled ambient room temperature of 23±1°C.

Table 0.4 OWC slurries mixed with Dura-Pozz

OWC slurries mixed with Dura-Pozz (classified FA – 90% < 45μm)						
Fly ash addition	%	2.5	7.5	15	20	30
Water	g	461	480	508.4	530	564.1
Cement	g	1500	1500	1500	1500	1500
FA	g	37.5	112.5	225	300	450
Additive	g	1.6	1.6	1.6	1.6	1.6
Total cementitious	g	1537.5	1612.5	1725	1800	1950
w/c ratio	g	0.300	0.298	0.295	0.294	0.289

Table 0.5 OWC slurries mixed with Super-Pozz

OWC slurries mixed with Super-Pozz (classified FA – 90% < 11μm)						
Fly ash addition	%	2.5	7.5	15	20	30
Water	g	480	480	517	522.8	564.3
Cement	g	1500	1500	1500	1500	1500
FA	g	37.5	112.5	225	300	450
Additive	g	1.6	1.6	1.6	1.6	1.6
Total cementitious	g	1537.5	1612.5	1725	1800	1950
w/c ratio	g	0.312	0.298	0.300	0.290	0.289

3.11 Slurry curing process

Once the casting process is completed, the slurry prism should be prevented from premature drying and temperature variation should be avoided. These precautions are put in place in order to protect the slurry prism from negative impact on methods of curing (Askar, et al., 2013). The slurry prisms should first be kept in a curing room (at controlled temperature and 90% humidity) for 24 hours before curing at elevated temperatures begins. In this study, two methods of curing were used as follows:

- Boiling water curing method
- Steam cured one day after casting

All slurry prism samples were placed in the laboratory (lab) for 24 hours to complete the process of hardening as indicated in Figure 3.15. The samples were then demoulded carefully. The weight of each sample was recorded after demoulding as indicated in Figure 3.16. After demoulding, the samples were immersed in water until the finishing operation was completed after 2 days, 7 days or 28 days.

Figure 0.15 Sample demolding process

Figure 0.16 Slurry prism weighing process

3.11.1 Steam cured method

In the steam- cured process, the sample prisms were first kept in a curing room (at controlled temperature and 90% humidity) for 24 hours before being steamed at 60°C.

3.11.2 Boiling water method

In the boiling water curing method; the slurry samples were initially moist-cured in the laboratory for 24 hours. After 24 hours had elapsed, the sample prisms were lowered into the boiling curing tank where they were maintained at 85°C for period of 2 days, 7 days or 28

days prior to compressive strength testing. The samples were immersed in water until completing the curing ages for specific samples tests.

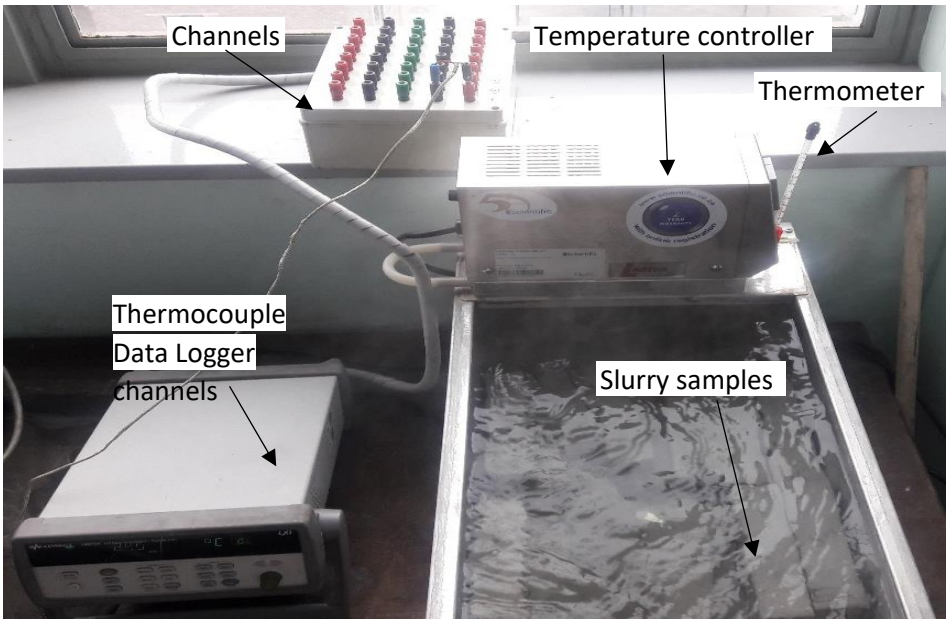

Figure 0.17 The boiling water process

In order to avoid a sudden change in temperature, the samples were transported to a compressive strength testing site by means of a temperature controlling cooler box as indicated in Figure 3.18, once the laboratory curing process was completed. The total time for cooling and breaking the prisms was 30 minutes for 2-days prisms, 2 hours for 7- days prisms and 8 hours for 28 - days prisms.

Figure 0.18 The samples transportation method

3.12 Compressive strength test

An automatic cement strength testing machine called the Tonicomp III with a capacity of 1600 kN was used and the load was applied at a rate of 3 kN/s. The compressive strength tests were performed according to SANS 5863:2006 on each of the three slurry prisms of (40 x 40x160) mm, for each cement-FA mix at 16 hours 2days, 7days, and 28 days of curing. The compressive strengths recorded from each of these tests were averaged for the 3 prisms as per SANS 5863:2006 (Msinjili & Schmidt, 2015).

Figure 0.19 The compressive strength testing process

CHAPTER 4: RESULTS AND DISCUSSION

4.1 Introduction

This chapter discusses the results obtained from the test of soundness, the characterization of the OWC samples, Eskom and Sasol coal fly ash (FA) samples using XRD, XRF, SEM, TGA, and PSA. Parameters considered were rheology and compressive strength. All tests were done according to API specifications. A comparison of the results from this study with results previously reported in literature is also made. Since most standards limit the carbon content of fly ash to 5% while a few allow values as high as 7% (Sankaranarayannan & Jagadesan, 2016). It is for this reason that Eskom coal fly ashes, Dura-Pozz and Super-Pozz were selected for preparing slurry cast test specimens due to their low carbon content as indicated by the % LOI in Table 4.3. The coal fly ash from Sasol and the Pozz-Fill from Eskom were not cast due to the limited OWC available.

4.2 Test of Soundness of OWC

The data collected as per Table 4.1 show an expansion in cement sample 1 and sample 2 of OWC. After cooling, the displacement of the mould arms for the first sample returned to its initial distance of 5mm.

Table 0.1 Soundness of OWC

Date	8/3/2019	Sample ID	OWC
Sample Description			
Balance ID	3402126	Mixer ID	LM1
Time ID	WC4	Le Chatelier moulds	L17
Ruler ID			
Expansion (c) - (a)	mm	mm	
AVERAGE	0	mm	
	1	2	
Distance after curing (a)	5 mm	5 mm	
Time placed on hot plate (f)	13:19	13:19	
Time started to boil (g)	13:50		
Time to boil (g-f)	(25 to 35 min)		
Time removed (h)	H:16:19		
Time boiled (h-g)	(175 to 185 min)		
Distance after boiling (b)	6 mm	6 mm	
Distance after cooling c	5 mm	6mm	

4.3 Test of Soundness of OWC & FA

The data collected as per Table 4.2 show an expansion indicated by the displacement of mould

arms. After cooling both samples returned to the initial distances of 9 mm and 7mm.

Table 0.2 Soundness of OWC & FA

Date	8/3/2019	Sample ID	OWC & FA
Sample Description			
Balance ID	3402126	Mixer ID	LMX
Time ID	WC4	Le Chatelier moulds	LMAA
Ruler ID			

	1	2
Distance after curing (a)	9 mm	7 mm
Time placed on hot plate (f)	13:19	13:19
Time started to boil (g)	13:50	
Time to boil (g-f)	(25 to 35 min)	
Time removed (h)	H:16:19	
Time boiled (h-g)	(175 to 185 min)	
Distance after boiling (b)	10 mm	9 mm
Distance after cooling (c)	9 mm	7 mm
Expansion (c) - (a)	0 mm	0 mm
AVERAGE	0 mm	

4.4 XRF analysis of OWC and FA samples

Table 0.3 XRF analysis of OWC and various FA used in this study

	OWC %	**Sasol %**	**Dura-Pozz %**	**Super-Pozz %**	**Pozz-Fill %**
SiO_2	22.63	46.26	52.83	52.29	56.08
Al_2O_3	3.32	25.02	33.46	32.78	29.95
Fe_2O_3	4.63	4.62	3.29	3.32	3.27
CaO	63.63	7.81	3.89	4.22	4.48
MgO	1.48	2.41	1.02	1.17	1.05
K_2O	0.40	0.81	0.62	0.71	0.66
Na_2O	0.25	0.69	0.33	0.29	0.19
TiO_2	0.36	1.42	1.64	1.68	1.53
Mn_2O_3	0.07	0.08	0.04	0.04	0.04
P_2O_5	0.06	0.72	0.31	0.55	0.43
SrO	0.08	0.04	0.05	0.05	0.04
SO_3	1.98	0.69	0.14	0.27	0.11
LOI @ 950°C	0.99	0.81	0.92	0.76	0.88
Sum %	99.88	91.38	98.54	98.13	98.71

The XRF results seen in Table 4.3 showed comparable Fe_2O_3 and MgO contents between OWC and FA. The purpose of adding fly ash is to utilise the SiO_2 in the ash in the pozzolanic reaction, forming CSH. The addition of fly ash will normally reduce early strength but results in higher strength of the cement/fly ash blend at later ages (from 28 days) through the pozzolanic reaction. Based on the oxide composition of coal fly ash, a leaching process can be used to ultilise the SiO_2 in the pozzolanic reaction and impregnation method can assist in increasing the amount of CaO (Sedres, 2016). The low SiO_2 in Sasol fly ash contributed the overall low sum of 91.38%.

4.5 Oxide content of class G cement

A Portland cement with similar chemical composition to class G oil well cement (OWC) was used for this study and this was achieved by means of an additive (LSM). Its chemical composition from X-ray fluorescence (XRF) analysis, is presented in Table 14 and the derived Bogue phase compounds in Table 4.5. The compounds considered are $4CaO.Al_2O_3.Fe_2O_3$, $3CaO.Al_2O_3$, $2CaO.SiO_2$, $3Ca.SiO_2$, uncombined MgO, uncombined CaO and $CaSO_4$. Other components than those included in these compounds are not at present considered as their forms of combination are unknown (Bogue, 1929). The phase composition derived using the modified Bogue calculation indicates C_3A in the cement from literature below 3 %, in line with the API Class G specifications (El-Gamal, et al., 2017; Deng, et al., 2002) . A value of 0.95 C_3A was recorded in Table 4.5 for the test OWC. Table 4.4 further shows the XRF results of the test OWC compared with previous literature. It can be observed that results obtained from the test OWC are almost similar and consistent with previous research conducted on ageing of oilfield cement (Deng, et al., 2002) and El-Gamal, et al., 2017.

Table 0.4 XRF analysis of Test OWC compared with literature

Composition %	Test OWC	OWC (Egypt) El-Gamal, et al., 2017	Deng, et al., 2002	API Class G OWC
SiO_2	22.63	21.80	22.52	
Al_2O_3	3.32	2.90	3.86	
Fe_2O_3	4.63	4.81	4.64	
CaO	63.63	64.90	63.53	
MgO	1.48	1.30	0.73	< 6.0
K_2O	0.4	0.33	0.71	
Na_2O	0.25	0.09	0.16	
TiO_2	0.36	-	0.18	
Mn_2O_3	0.07	-	0.17	
P_2O_5	0.06	-	0.05	
SrO	0.08	-	0.16	
SO_3	1.96	-	0.37	$\leq$ 3.0
LOI @ 950°C	0.99	0.80	-	
Sum %	99.87	96.93	97.08	

Table 0.5 Bogue phase calculation derived from XRF data compared with literature

Phase Mass %	OWC	El-Gamal, et al., 2017	Deng, et al., 2002	API Class G OWC
Alite (C_3S)	**58.07**	**63.70**	**60.50**	**48-65**
Belite (C_2S)	**21.09**	**13.50**	**21.40**	
Tricalcium aluminate (C_3A)	**0.95**	**0.00**	**2.39**	**< 3.0**
Tetracalcium aluminoferrite (C_4AF)	**15.99**	**14.60**	**19.10**	
C_4AF + 2 C_3A	**16**			**<24**

4.6 Chemical composition of FA using XRF

Table 0.6 Chemical analysis of test FA samples compared with literature

Component	Sasol %	Dura-Pozz %	Super-Pozz %	Ayanda, et al., 2012
SiO_2	46.26	52.83	52.29	51.43
Al_2O_3	25.02	33.46	32.78	30.93
Fe_2O_3	4.61	3.29	3.32	2.29
CaO	7.80	3.89	4.22	6.75
MgO	2.41	1.02	1.17	1.95
K_2O	0.81	0.62	0.71	0.77
Na_2O	0.69	0.33	0.29	0.54
TiO_2	1.42	1.64	1.68	1.74
Mn_2O_3	0.08	0.04	0.04	-
P_2O_5	0.72	0.31	0.55	1.08
SrO	0.04	0.05	0.048	-
SO_3	0.4	0.10	0.112	-
LOI	0.69	0.15	0.27	1.21
Sum %	90.95	97.73	97.48	98.69

4.7 Crystallinity of OWC using XRD

An equivalent, Class G oil well cement (OWC) (in accordance with the American Petroleum Institute (API) specification) was used in laboratory tests. The cement composition is shown in Table 4.4, determined by X-ray fluorescence (Bruker S8 Tiger XRF spectrometer).

Below, its mineralogical phase compositions as measured by powder XRD using a Brucker D2. PHASER. X-ray diffractometer are shown in. Figure 4.1. The patterns indicate that the OWC has C_S type phases which is consistent with previous research by Saout, et al., 2006. The presence of unhydrated phases alite C_3S, belite C_2S, and tetracalcium aluminoferrite C_4AF is demonstrated.

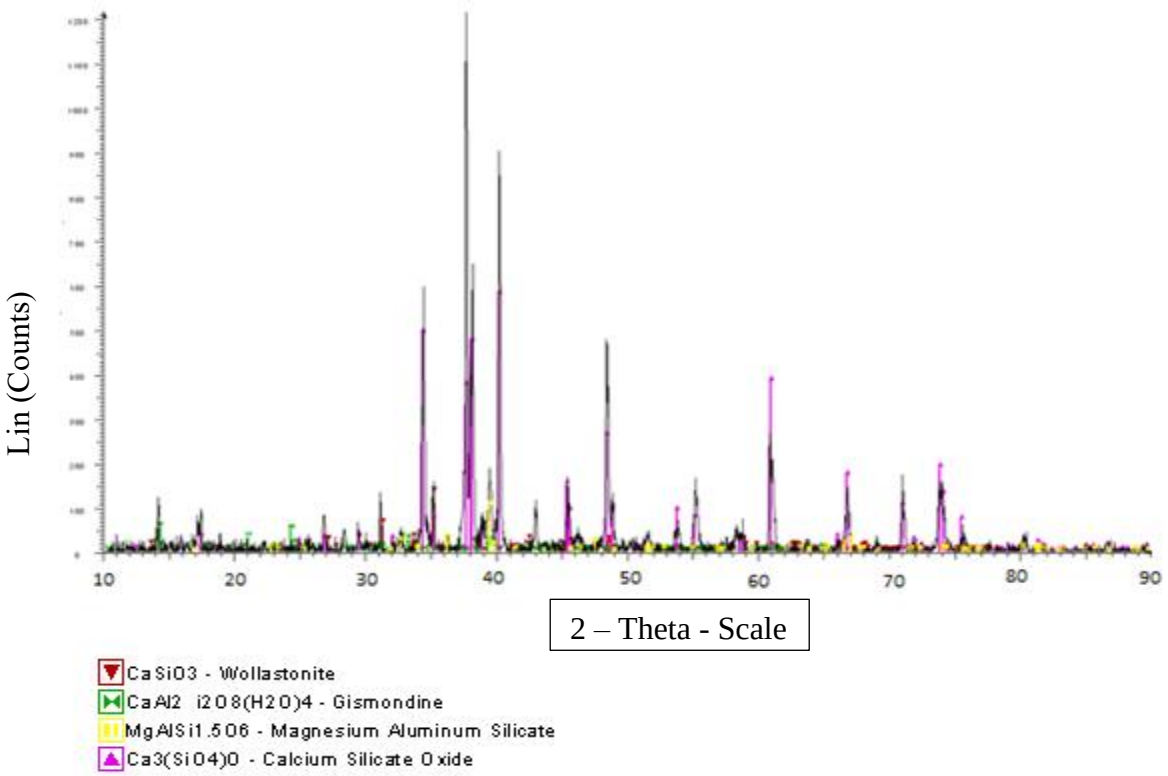

Figure 0.1 XRD Diffractogram of OWC

4.8 Crystallinity of FA using XRD

X-ray diffraction (XRD) was used to identify crystalline phases in the FA. Powdered samples were analysed on glass slides at angles between 0° and 60°, the positioning of the angle was similar to Duguid and Scherer (2010). Figure 4.2 shows the XRD patterns of Sasol FA. The patterns illustrate that the dominant phases are alpha quartz (SiO_2) and mullite Al.83Si1.0804.85 (a silicate mineral with various Al to Si ratios). Traces of calcite, $CaCO_3$ (Calcite -0.1-086-2340) were also identified. The same phases were identified in a previous study on characterization of fly ash generated from Matla Power Station in Mpumalanga, South Africa (Ayanda, et al., 2012). A much clearer quantitative understanding was achieved with XRF analysis.

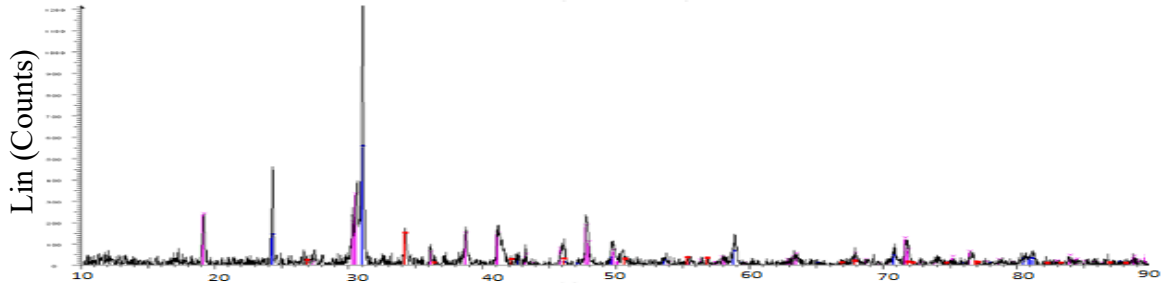

Figure 0.2 Crystallinity of Sasol FA using XRD

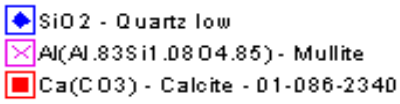

Figure 4.3 and Figure 4.4 both show XRD patters of FA. The crystalline phases of the FA can be identified qualitatively by means of XRD. The major and minor crystalline phases can also be identified with a high intensity scan. A major match involves the match of 3 peaks of a particular phase (Kruse, et al., 2013). In Figure 4.3 and Figure 4.4, the dominant phases are quartz (SiO_2) and Mullite – (Al.83Si1.0804.85). Traces of Dolomite – CaMg $(CO_3)_2$ are also found. Similar phases to those in both Figures were identified in previous research by Ayanda, et al., 2012.

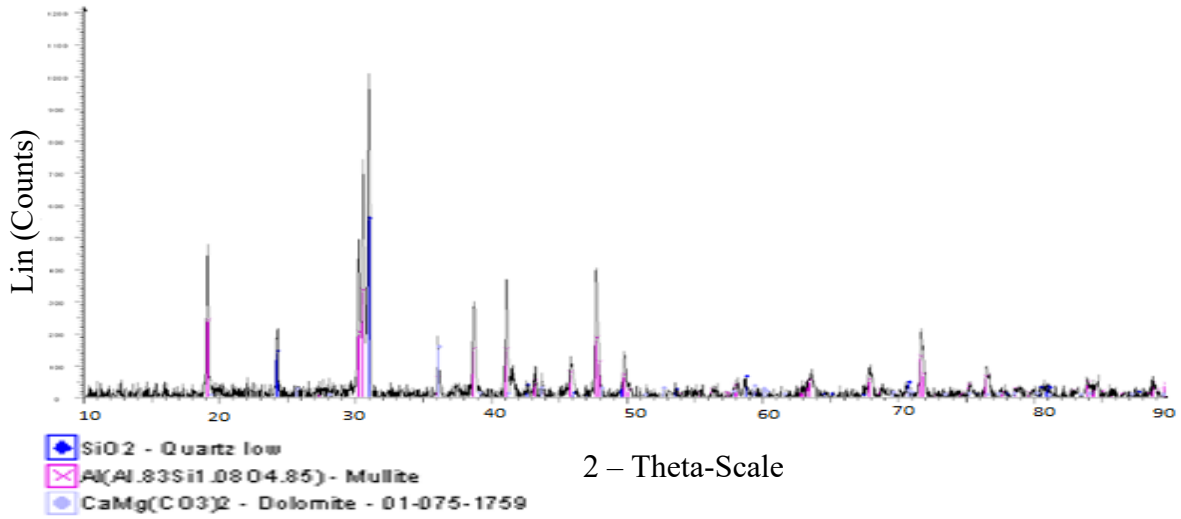

Figure 0.3 Crystallinity of Dura-Pozz FA using XRD

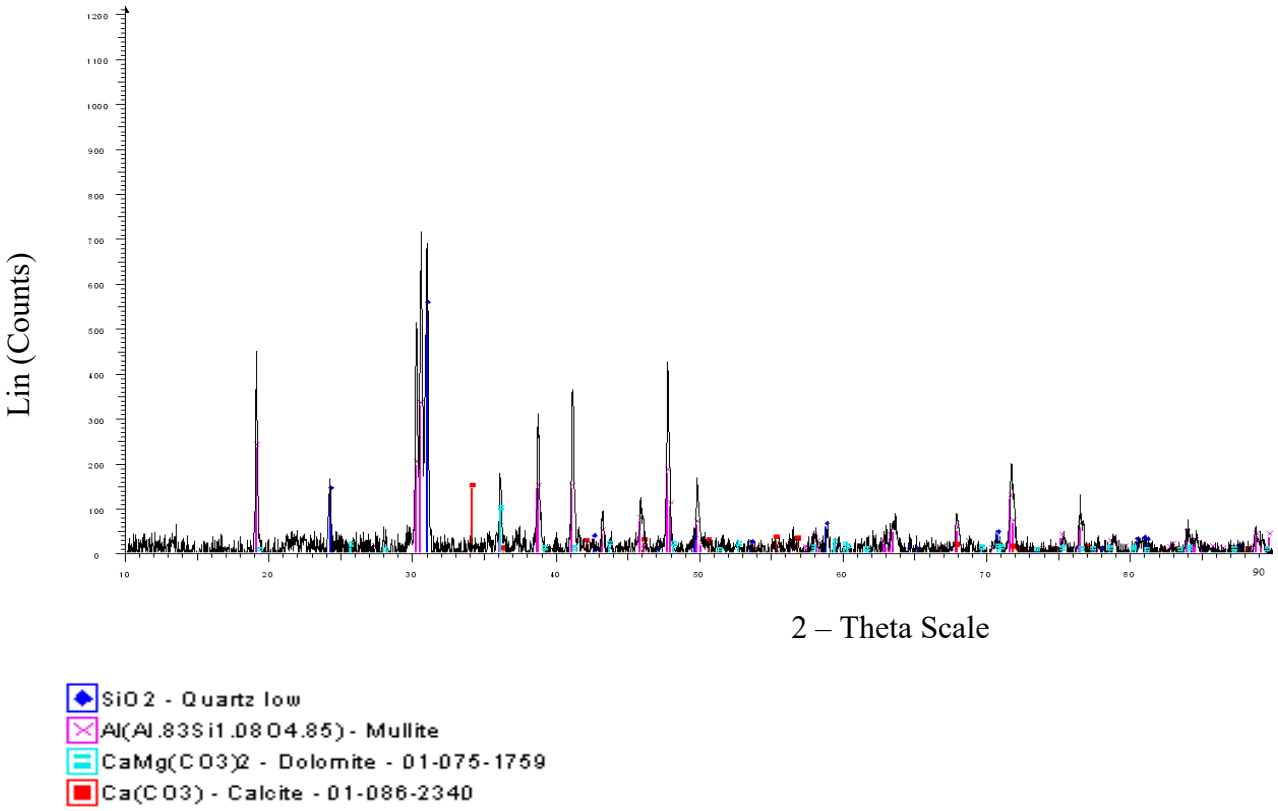

Figure 0.4 Crystallinity of Super-Pozz FA using XRD

4.9 Morphology of OWC using Scanning Electron Microscopy (SEM)

The morphology of the OWC is depicted in the Scanning Electron Microscope (SEM) micrograph in Figure 4.5. The shapes are similar to those observed in the hydration of class G oil well cement (Lota, 1993). As seen in Figure 4.5, most of the particles are smooth with irregular hexagon shapes, as seen at higher magnifications. A similar observation has been reported by Lota et.al 1993. The SEM micrograph depicts a high level of calcium when compared to other chemical elements and this is consistent with previous report on class G oil well cement by Deng, et al., 2002.

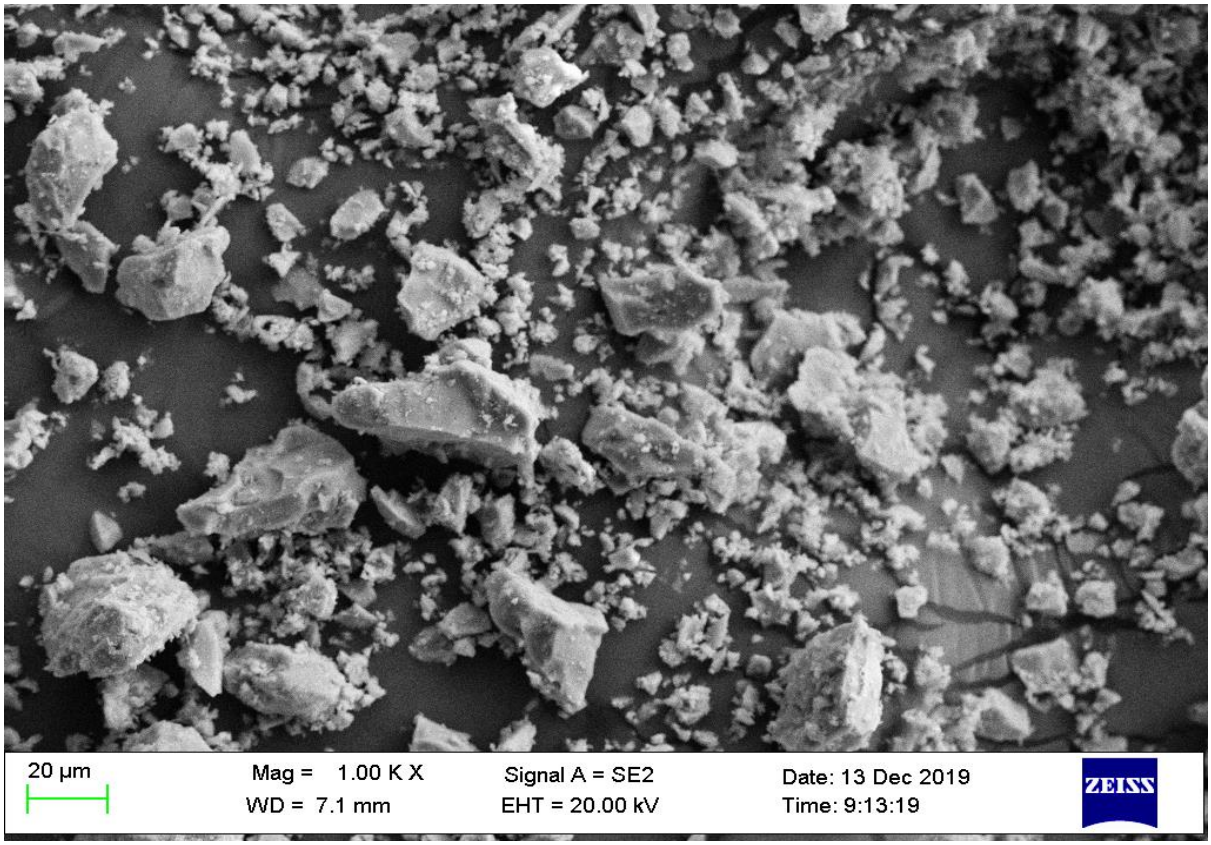

Figure 0.5 SEM micrograph of OWC

4.10 Morphology of FA using SEM

The Sasol, Dura-Pozz and Super-Pozz FA samples studied under the SEM proved to consist of Cenospheres, Plerospheres and agglomerates, as a result of bituminous coal combustion properties. (Apostolidou & Georgakopoulos, 2018). A Plerosphere is a cenosphere which may contain a mass of microspheres (1 µm or less in diameter) and in general it may be coated with silica (Apostolidou & Georgakopoulos, 2018). According to Kaduku, et al., 2015, the shapes of the FA particles are determined by their exposure conditions based on the actual time and temperature regulation in the combustion chamber.

The morphology of the FA samples is shown in the SEM micrographs in Figure 4.6 - 4.8. As seen in Figure 4.6, most of the Sasol FA particles are spherical and some have hexagon shapes, as seen at higher magnifications. A similar observation has been reported by Apostolidou at el, 2018 and Ayanda et al, 2012. The particles are a combination of opaque and non-opaque spheres. The opaque spheres are mainly iron oxides and some silicates whereas the non-opaque spheres are mainly silicates (Kaduku, et al., 2015).

In some cases, these are made up of smaller particles which are attached to the surface of bigger particles, hollow spheres (cenospheres), and some spheres containing other spheres (plerospheres). In addition, the SEM micrograph shows the presence of some non-spherical particles. Some particles are non-spherical as a result of incomplete combustion of coal components that were not exposed to high temperatures (Kaduku, et al., 2015).

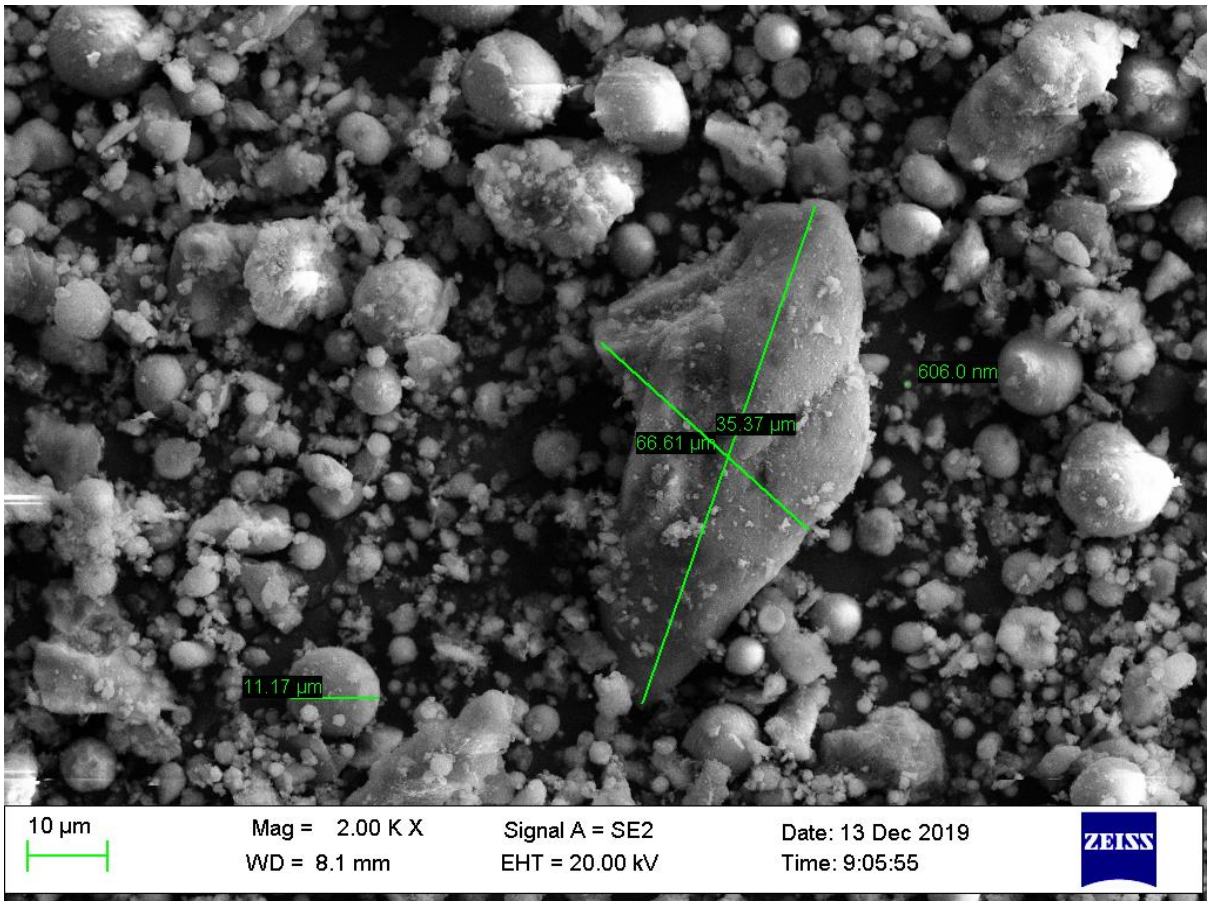

Figure 0.6 Morphology of Sasol FA using SEM

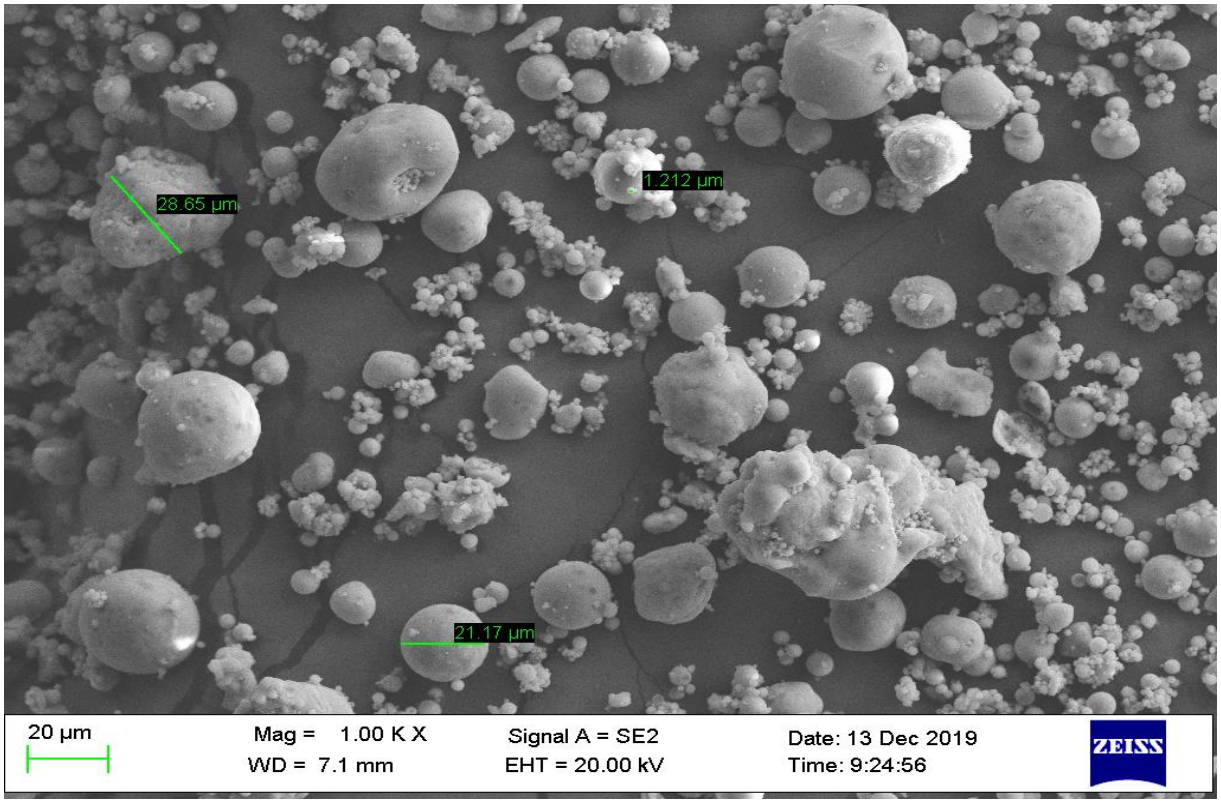

Figure 0.7 Morphology of Dura-Pozz FA using SEM

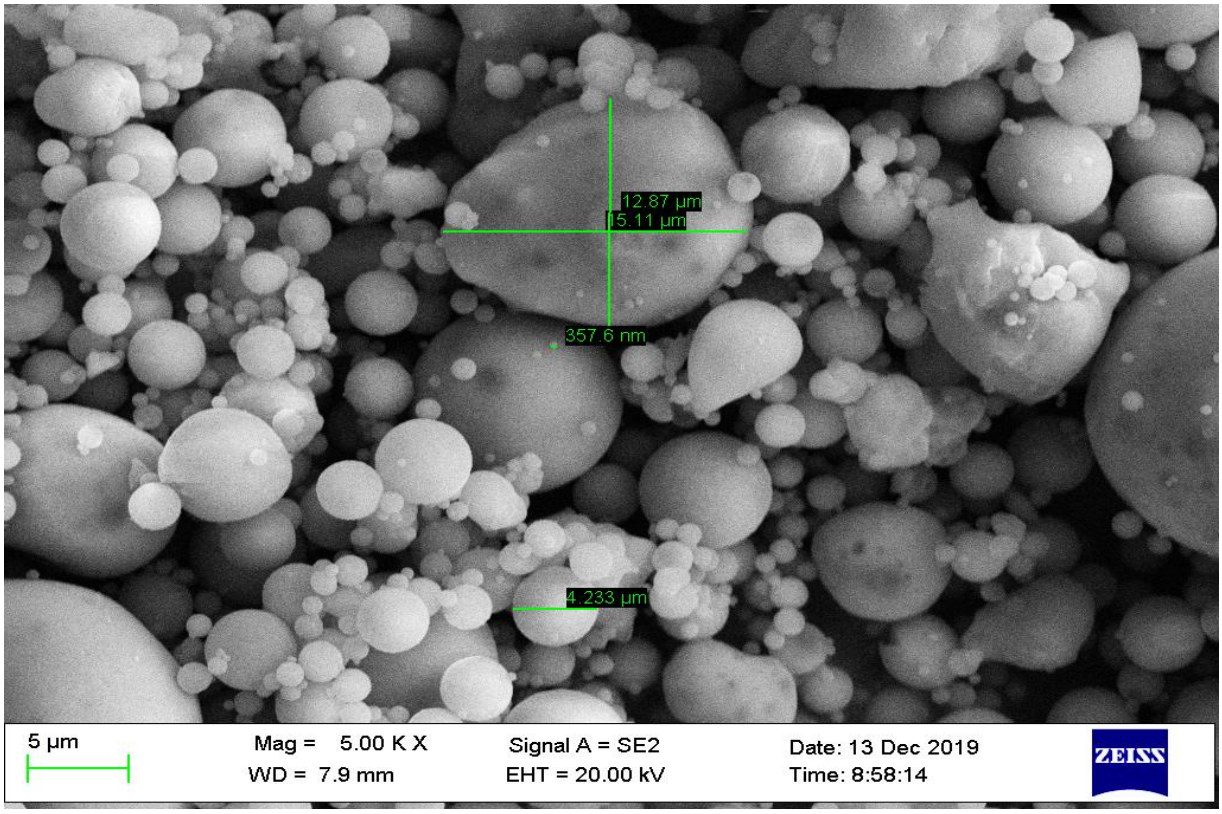

Figure 0.8 Morphology of Super-Pozz using SEM

4.11 Proximate Analysis and pH of FA samples

The proximate analysis of coal and coal derived products using modern thermogravimetric analysis (TGA) is extensively used by coal ash users primarily due to the speed of analysis. In this case, a coal ash specimen may be analysed for percentage moisture, fixed carbon, total volatiles and ash residue in less than 30 minutes (Earnest, 1988). The results reported in Figure 4.9 showed that Super-Pozz contains 0.8% moisture, 6% volatile matter and 2% fixed carbon.

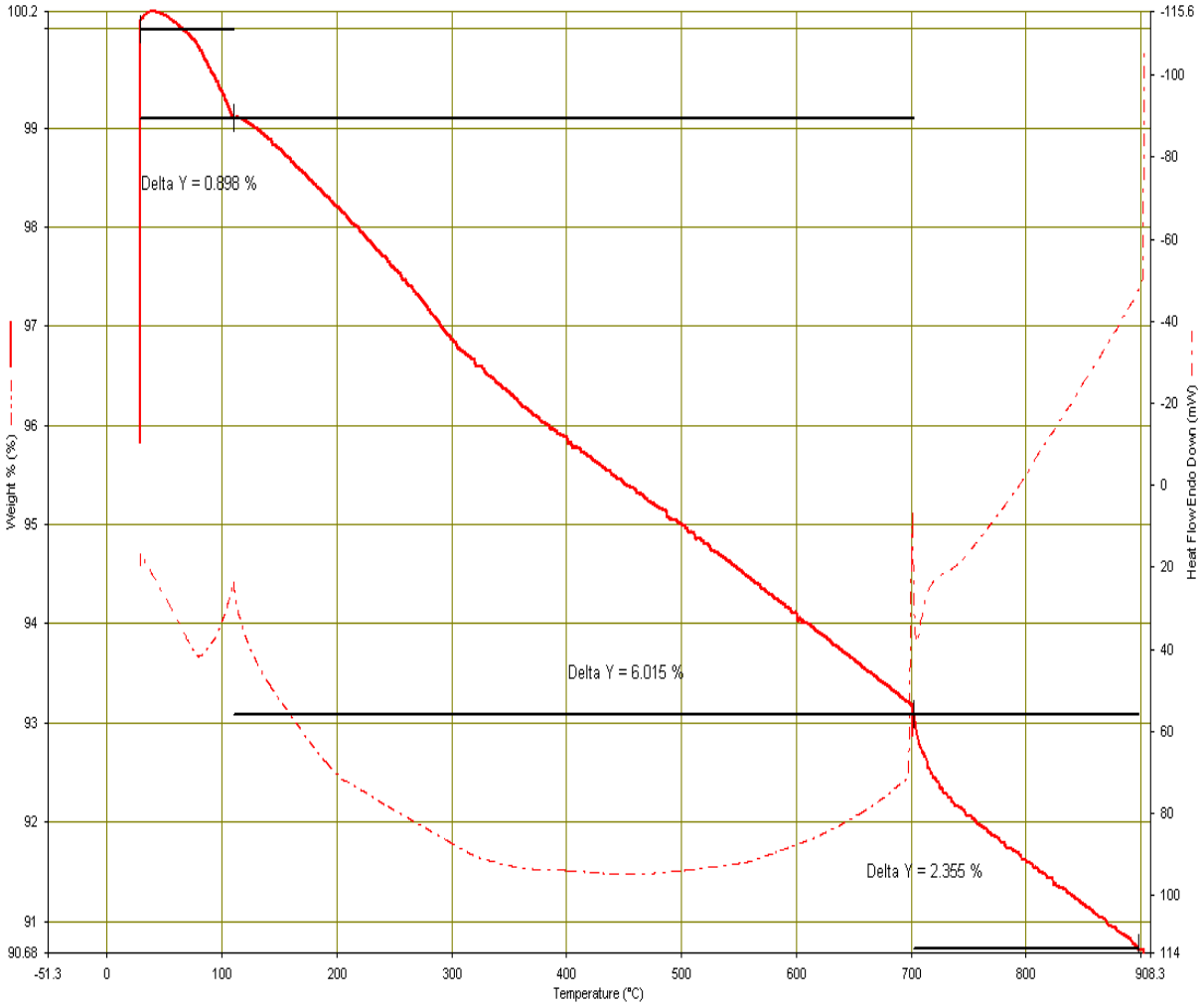

Figure 0.9 Thermogravimetric Analysis of Super-Pozz FA

In general, a rise in pH from 7 to 10.12 was observed when the FA was mixed with de-ionized water over a period of 5 hours. The Super-Pozz FA reached a maximum pH of 10.12 while the Dura-Pozz FA pH was 9.90. In comparison, the OWC sample reached a maximum pH of 10.10.

4.12 Particle size analysis

Table 0.7 Laser Diffraction Analysis Data

Parameter		**OWC**	**Dura-Pozz**	**Super-Pozz**	**SASOL**
D (0.1) (10% passing)	**(µm)**	5.28	4.63	0.50	4.37
D (0.5) (50% passing)	**(µm)**	19.35	12.16	6.70	18.05
D (0.9) (90% passing)	**(µm)**	49.90	30.85	19.32	50.21
Surface weighted mean D (3.2)	**(µm)**	12.09	9.39	1.53	10.56
Volume weighted mean D (4.3)	**(µm)**	24.12	15.32	8.89	23.21
Specific surface Area	**(m^2/kg)**	496	640	3927	569

From Table 4.7, it can be seen that – except for the Sasol sample - the weighted residual of the investigated samples is less than 1% (Malvern Instrument Ltd, 2007), which is an indication of how well the detector calculated data fitted to the measurement data. This can also be seen on how the volume weighted mean of the investigated samples varied with the surface weighted mean.

The obscuration values show that the OWC and Sasol samples are coarse particles (5 – 12% obscuration); Dura-Pozz and Super-Pozz are polydisperse particles (14 – 20% obscuration). All values of obscuration are between 10 and 20%, which indicate an acceptable range of particle size (Malvern Instrument Ltd, 2007). It can also be seen that the surface weight mean and the volume weighted mean particle diameter of Super-Pozz is significantly smaller than the other investigated samples. Fly ash was used in blends with cement in various proportions. The data from the particle size distribution reveal the sizes that should be taken into consideration when mixing cement and fly ash.

4.13 Setting time rate comparison between OWC and OWC mixed with 30% fly ash

As a standard procedure, cement setting time is determined by the Vicat test. It measures the setting time by the decrease of needle penetration into the specimen with increasing structure formation (Zhang, et al., 2010). In Table 4.8, the initial setting time of OWC was 80 minutes. The OWC mixed with 30% FA, recorded an initial setting time of 197 minutes. The samples were mixed with water to a consistency of 26.86 % with 134 ml (OWC) and 25.66 % with 128

ml (OWC with 30% FA). The final setting time was achieved much quicker in OWC at a 0.0 mm penetration rate after 197 minutes as opposed to the OWC mixed with FA, which took significantly longer to achieve the 0.0 depth after 1099 minutes as indicated in Figure 4.10. Table 18 indicate the difference in water quantities in order to increase workability between OWC and OWC with 30%. The deviation from the setting time is due to the addition of FA which acted as a retarder by slowing the setting time process.

Table 0.8 Initial Set and Final Set

	Standard consistency (%)	Water (ml)	Initial set (min)	Final set (min)
OWC	26,86	134	80	170
OWC / 30% FA	25,66	128	197	1099

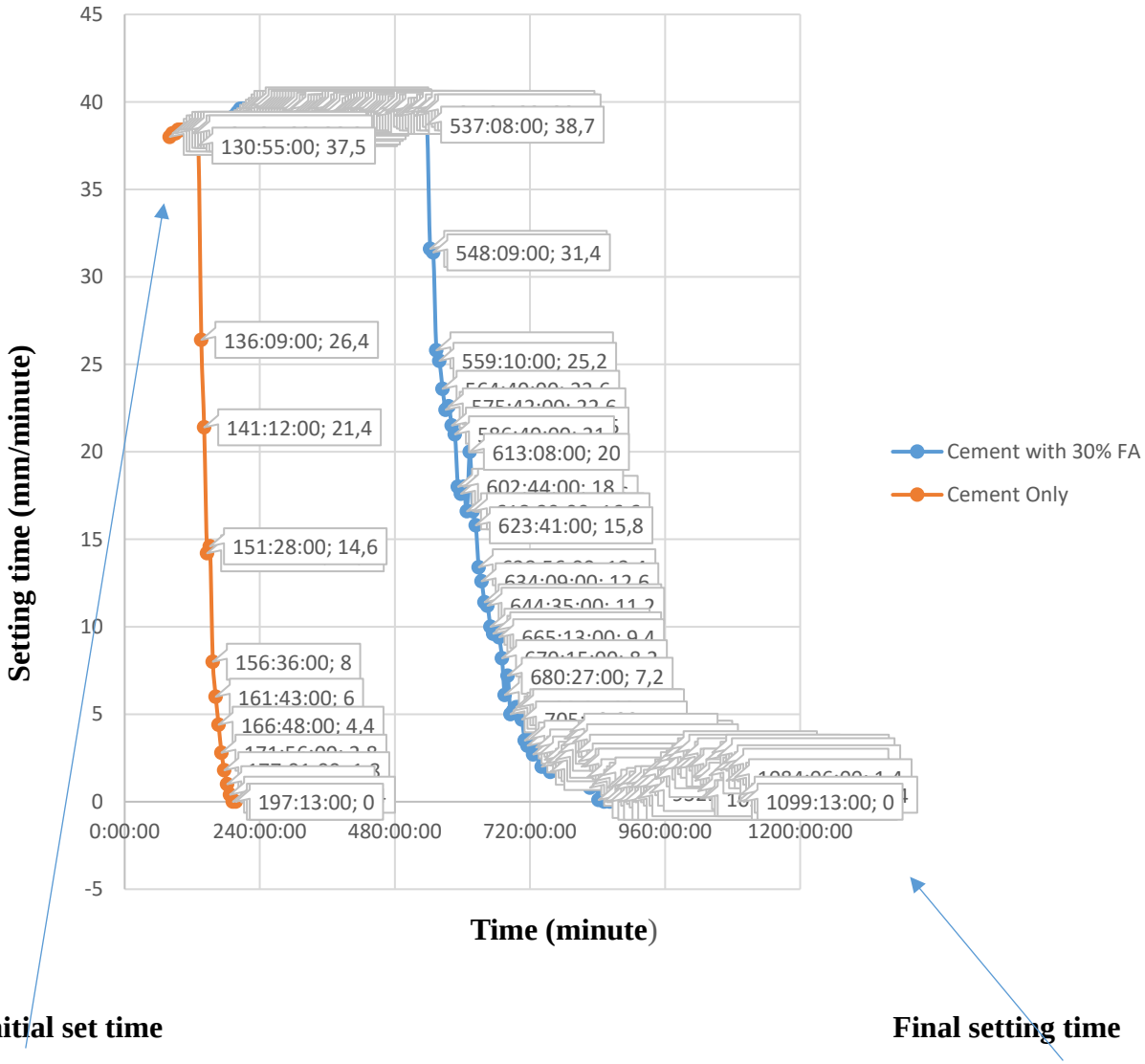

Figure 0.10 Comparative behaviour of setting rate between OWC & OWC with 30% FA

4.14 Rheology

The rheology of OWC pastes or slurries is generally more complex than that of Portland cement paste. In it resides the possibility to affect the primary oil well cementing job. In order to cope with bottom hole conditions (these may include a wide range of pressure and temperature), additives are used in the OWC slurries. These exhibit different characteristics depending on the combination of admixture used and for the purpose of this research, a lignosulphonate-based mid-range water-reducing admixture (LSM) was used (Shahriar, 2011).

Figure 4.11 shows the relationship between Apparent viscosity and shear rate at 25 ^{0}C. The apparent viscosity known to be the viscosity at a specific shear (Shahriar, 2011). It can be observed that the graph follow a normal relationship as reported by Shahria and Nehdi (2012) and shear thining can be observed. A shear thinning is regarded as a decrease in apparent viscosity as the shear rate increases (Shahriar, 2011). A slight change is observed though at point 0.84 of 0.5 viscocity percentage. This could be attributed to human error or machine calibration. Figure 4.12 shows the relation between viscosity and shear rate at 45 ^{0}C. This graph follow a normal relationship as observe by previous research conducted by Shahria and Nehdi (2012). The Apparent viscosity decreases as shear rate increases.

According to Yahia and Khayat (2001) it is almost impossible to capture all possible trends of flow behaviour by means of a single rheological model. Figure 4.13 as well shows the relation between two variables, apparent viscosity and shear at 60 ^{0}C. The rheology results in this graph follow an unpredicted behaviour where points at 0.5, 0.7, and 0.9 percent are not in agreement with the research conducted by Shahriar (2011);

At 25 ^{0}C and at 45 ^{0}C the rheology behaviour is similar where both graphs follow a consistent trend for the apparent viscosity of the different percentages of LSM ranging from 0.1 % to 0.9%. However, at 60 ^{0}C the rheology behaviour changes drastically and requires further investigation.

In general, LSM should be added with precaution depending on the expected viscosity. All investigated LSM concentration showed an exponential behaviour. But at higher temperature such as 60 ^{0}C and LSM concentration between 0.7, the viscosity had an exponential – dumping behaviour. This could be due to the interaction between particles due to the presence of LSM

and the strength stability of LSM with temperature as per the work done by Satiyawira et al, 2010. Further investigations should be needed in order to understand the dumping behaviour.

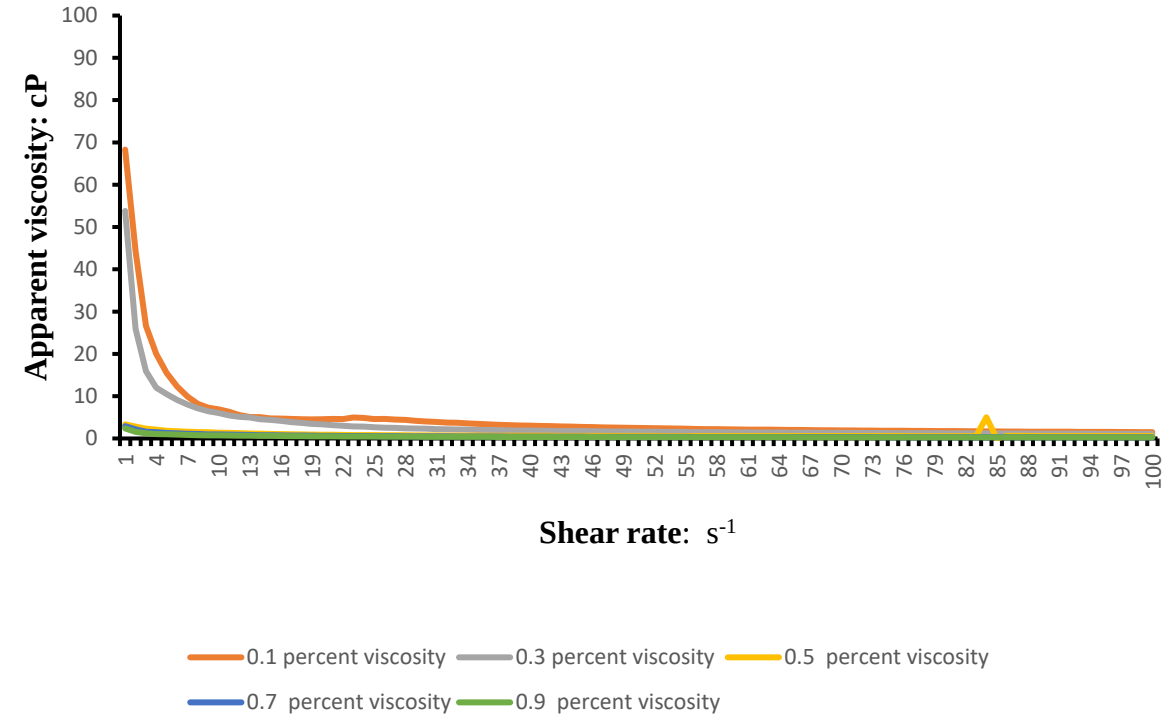

Figure 0.11 Rheology test at 25 °C (OWC with varying LSM dosage)

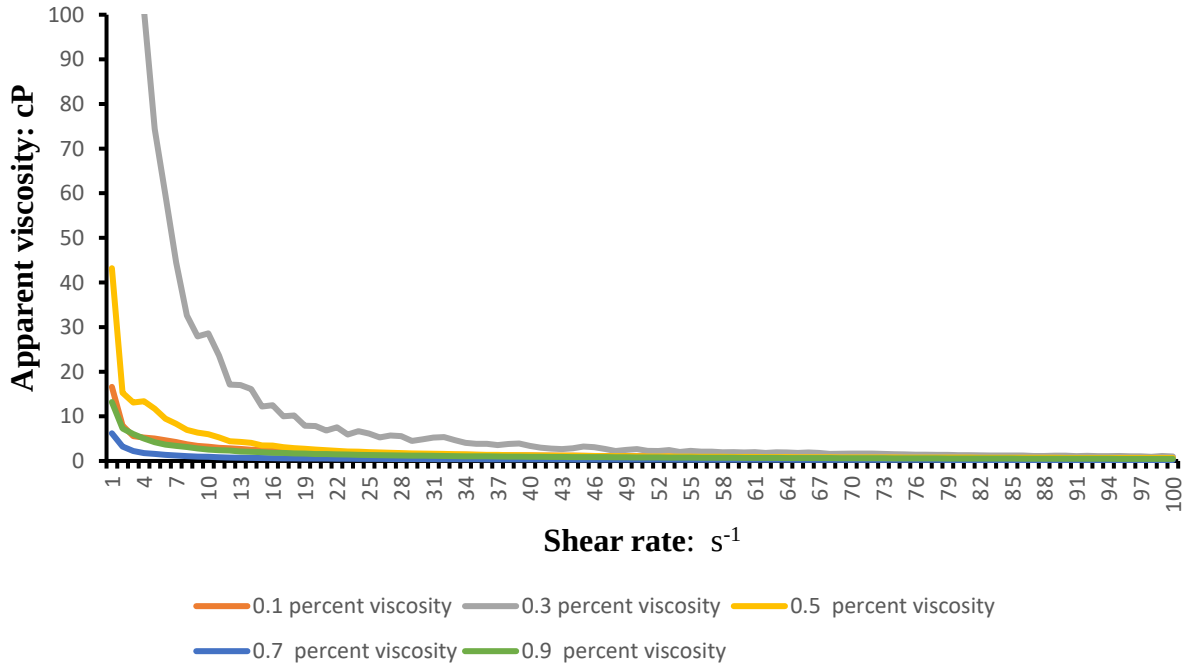

Figure 0.12 Rheology test at 45 °C (OWC with varying LSM dosage)

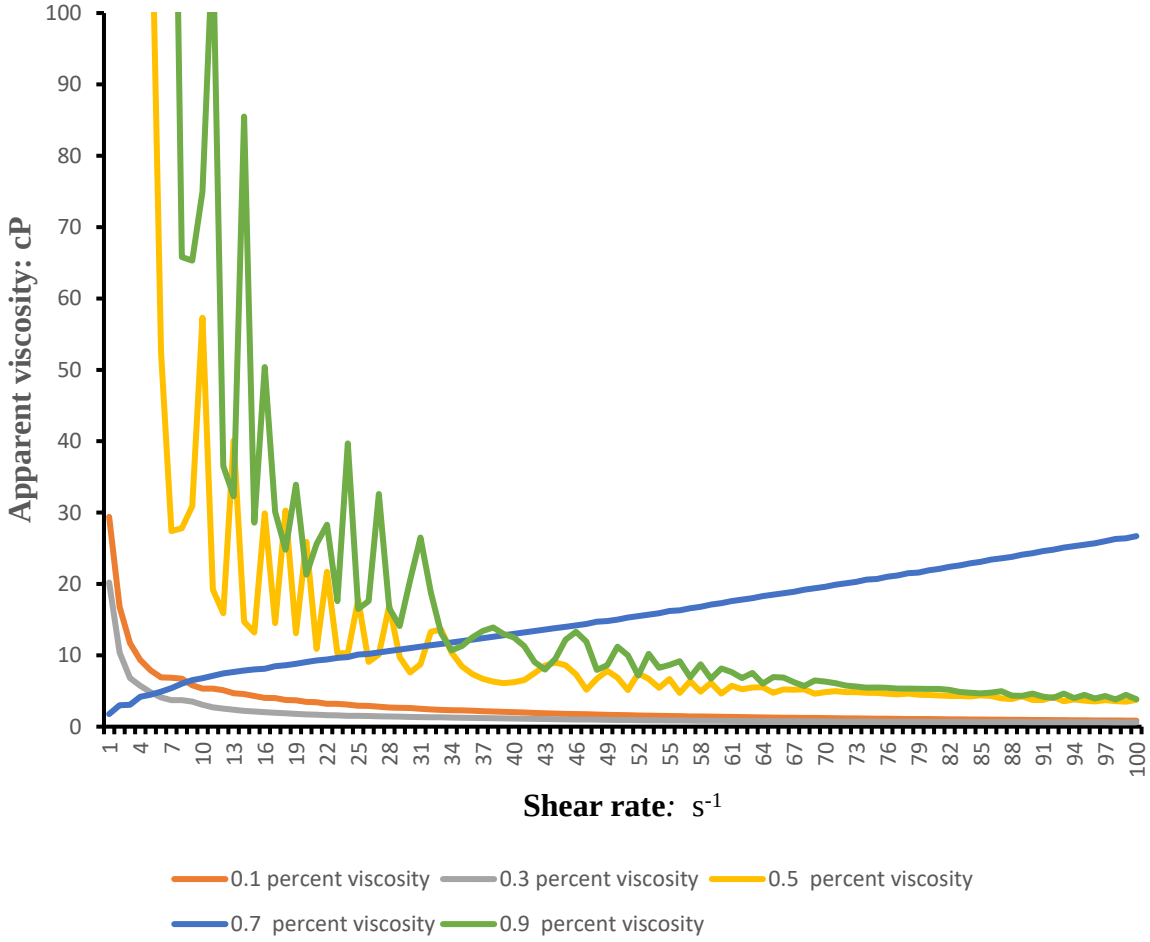

Figure 0.13 Rheology test at 60 °C

4.15 Compressive strength analysis

4.15.1 OWC combined with 30 % Dura-Pozz Steam Cured results analysis

The compressive strength test began with samples steam cured at 60 °C for 16 hours. For the purpose of this research only 4 samples where cast as per the appendix data. A mean compressive strength of 57 MPa was obtained.

4.15.2 OWC combined with Dura-Pozz results analysis

The compressive strength of cements plays a critical role in determining the overall quality. Increased durability is indicated by the higher compressive strength and lower porosity of a given sample (Broni-Bediako, et al., 2015). In an unlikely event of inadequate compressive

strength, casing failures are more likely to occur and life span of the well will be significantly reduced (Ridha, et al., 2013).

As per data attached in appendix, using the platens, the compressive strength was calculated from a 40x40mm area of each prism. The effective area in the compressive strength is therefore 1600mm^2. Figure 4.14 represent the results of compressive strength tests of cast slurries mixed with Dura-Pozz FA and LSM water-reducing admixture cured at ±85°C (185°F) for 2 days, 7 days and 28 days. It is evident that the increase in compressive strength after 2 days of curing in Figure 4.14, indicates early strength, and this is consistent with previous research done by Labibzadeh, et al., 2010 that looked at early-age compressive strength assessment of oil well class G cement. It explains that the development of high early-age compressive strength of OWC as an important task in the oil well cement design.

Achieving a suitable early-age compressive strength of oil well cement ensures both the structural support for the casing and hydraulic/mechanical isolation of borehole intervals (Labibzadeh, et al., 2010). After 7 days, it can be observed that the compressive strength increases with FA additions. The highest compressive strength was achieved after 28 days, and this corresponded to 7.5% FA addition as indicated in Figure 4.17. An anomaly in terms of

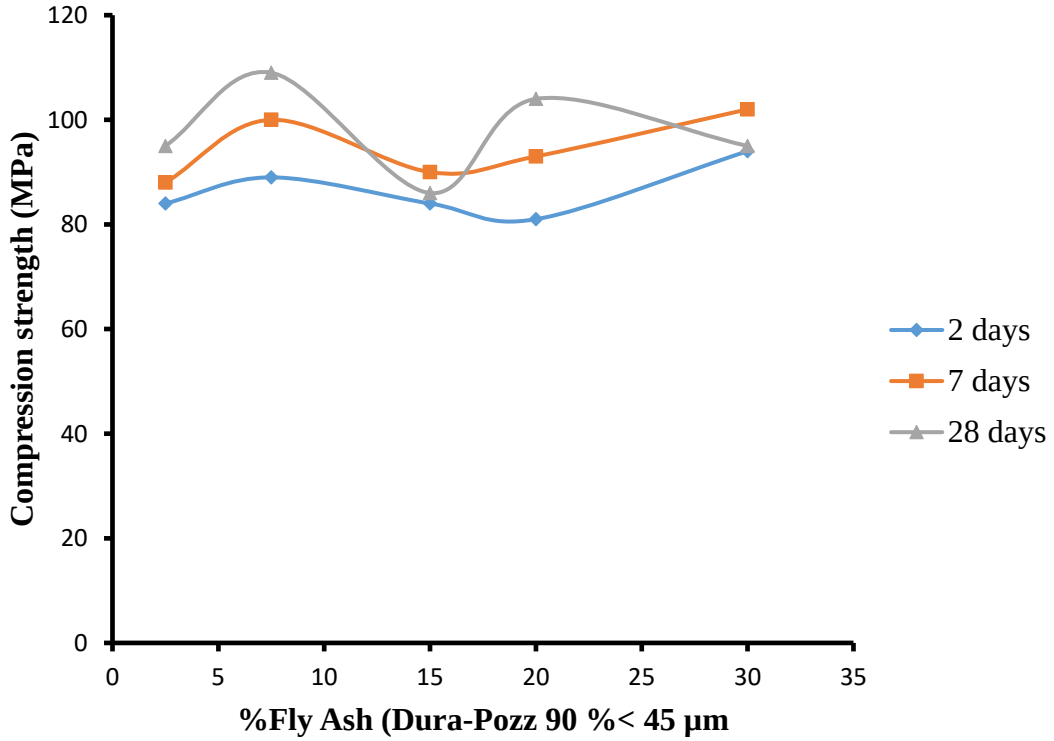

compressive behaviour has been observed with the addition of FA to the maximum of 30%. The 7 days and 2 day strengths are higher than the 28 days strength. The low strength was attributed to a drop in curing temperature caused by a failure in temperature control due to intermittent Eskom load shedding together with the planned power upgrade in the Richard Ward building over a 3 days. A similar anomaly can be observed with 15% fly ash, where the 7 days and 2 day strengths are also higher than the 28 days strengths. Further investigations are required in order to check these anomalies as compressive strength increases with time.

Figure 0.14 Effect of Dura-Pozz fly ash on oil well cement compressive strength

4.15.3 OWC combined with Super-Pozz results analysis

Figure 4.15 shows the result for compressive strength of OWC slurries mixed with LSM and Super-Pozz FA cured at ±85°C (185°F) for 2 days, 7 days and 28 days. After 2 days and 7 days, the compressive strength is relatively the same as those in Figure 4.14 and this is in agreement with previous research (Labibzadeh, et al., 2010). After 28 days, in contrast to Figure 4.14, a higher compressive strength corresponding to 15% of FA is recorded, and this is a clear indication of late strength in terms of cement. The hardened cement slurry must exhibit adequate compressive strength and chemical durability to withstand the pressure due to the reservoir formation and the deterioration due to the presence of attacking chemicals (Allahverdi, et al., 2013). Medium and late-age compressive strengths are essential, since they depend on the total amount of calcium silicate content (both alite and belite) of the cement which is a quality characteristic determining the properties of the cement including its durability performance under especial conditions (Allahverdi, et al., 2013).

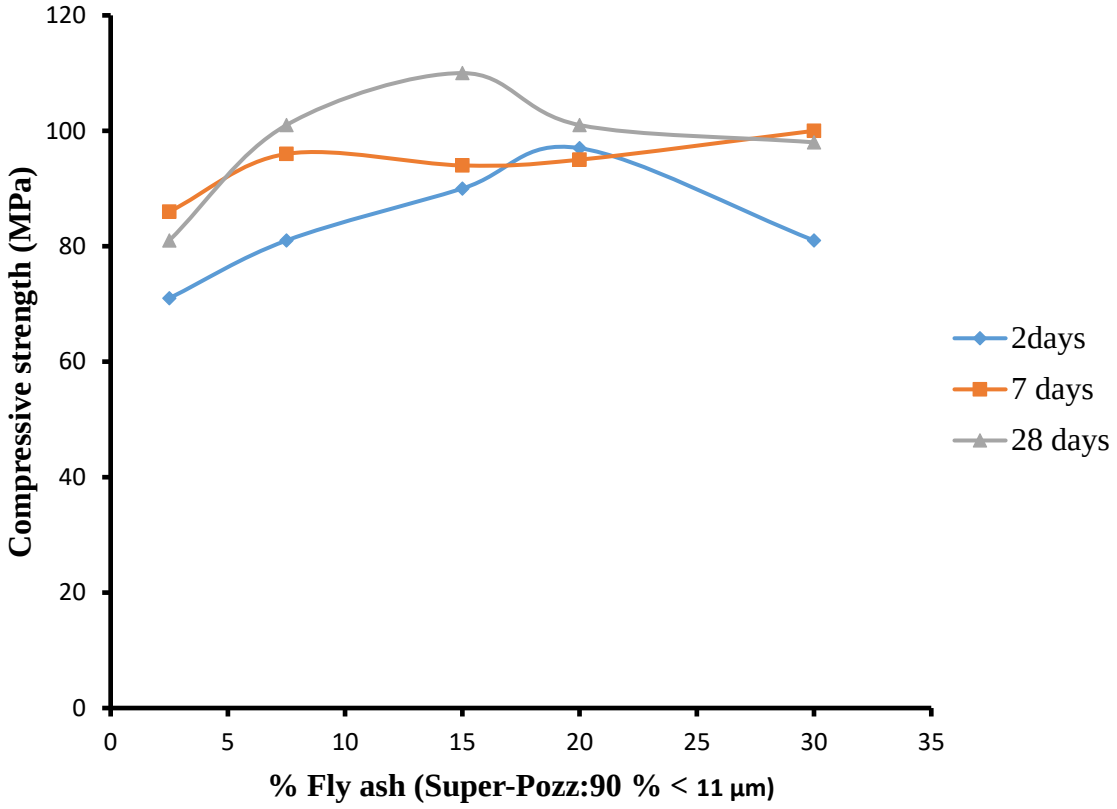

Figure 0.15 Effect of Super-Pozz- fly ash on oil well cement

4.15.4 Comparative behaviour of Super-Pozz and Dura-Pozz

Comparing the behaviour of the two plots, Figure 4.16 (comparison at 28 days) provides a clear indication of maximum compressive strength. Figure 4.16 shows that Superpozz increases in strength up to a stable compressive strength which confirmed the findings of Yazici et al., 2012. The compressive strength increase with the finesse of FA. Durapozz decreases in strength with a dumping behaviour. The particle size and the FA content had an effect on the compressive strength. The dumping behaviour should be investigated in the future.

The Super-Pozz graph recorded the highest peaks creating a big gap at 15% FA. At 20%, the gap between the Super-Pozz and the Dura-Pozz narrows in terms of compressive strength. This decrease in strength should be investigated in the future. At 30% increase FA by weight, Super-Pozz emerge to be the graph that has recorded the highest compressive strength at 28 days. The results obtained are similar to those from previous research that looked at high performance of

FA (Supit & Shaikh, 2014). The addition of 1% nano-silica fume of high volume fly ash (HVFA) increased the compressive strength at early ages (Faiz Shaikh, 2014).

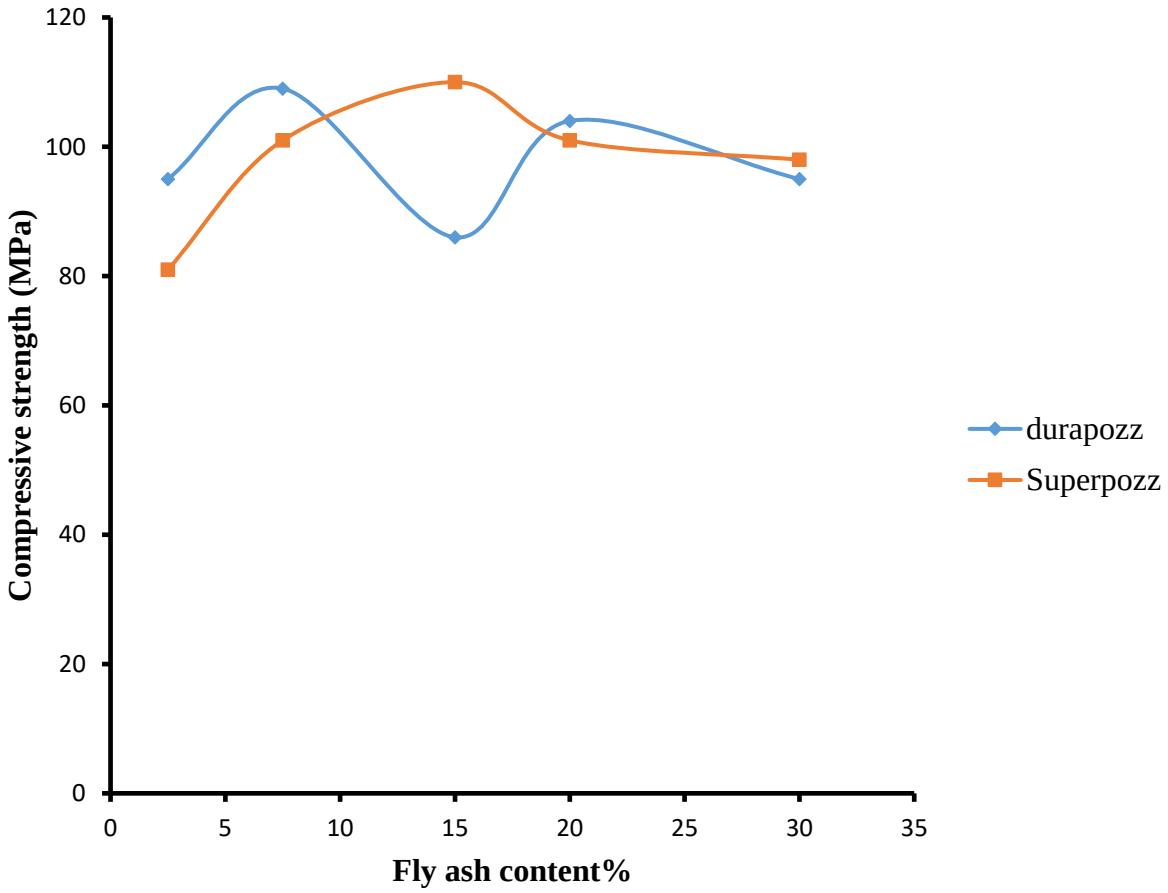

Figure 0.16 Comparative behaviour of Super-Pozz and Dura-Pozz at 28 days

4.15.5 Comparative behaviour of Super-Pozz and Dura-Pozz early strength

According to the API, Wait-On-Cement (WOC) can be defined as time required for cement to achieve a minimum compressive strength, which equals to 3.45 MPa (500 Psi), for resisting the shocks caused by drilling operation at later stages and in this instance the minimum compressive strength was recorded at 15% for Dura-Pozz at 43 MPa and for Super-Pozz, the minimum compressive strength was recorded at 2.5% at 41.4 MPa (Labibzadeh, et al., 2010).

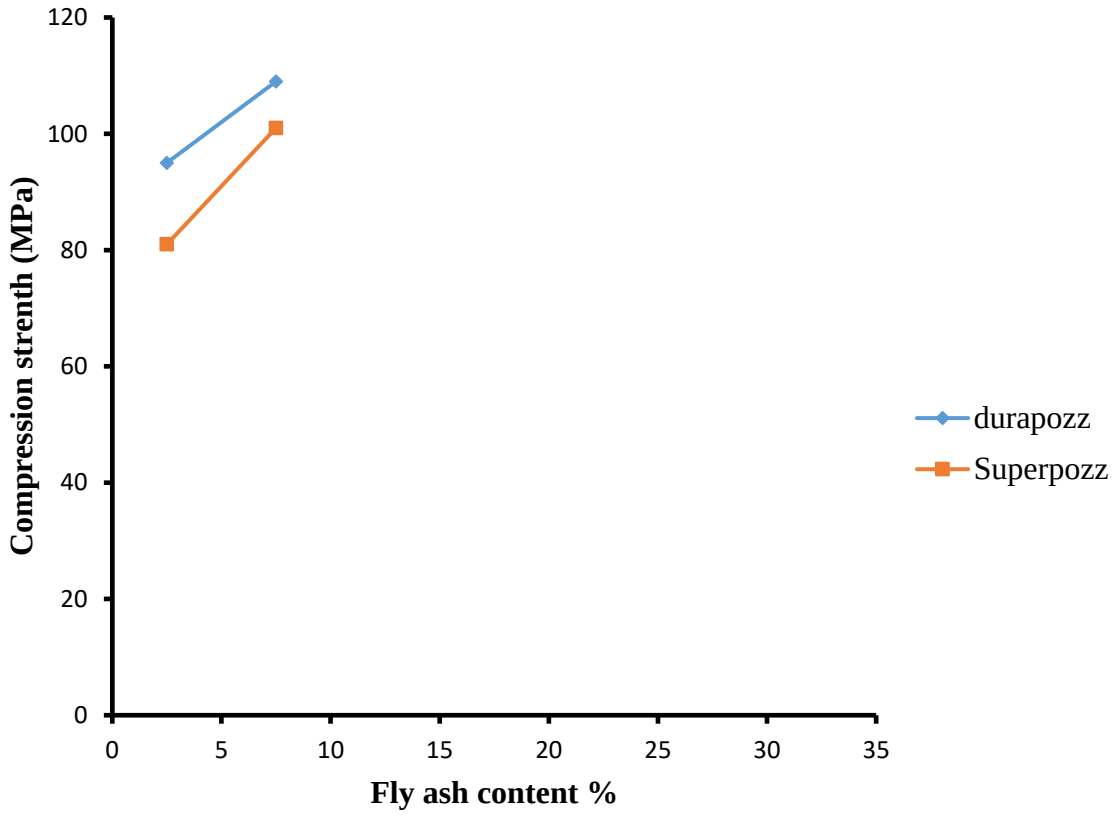

Figure 0.17 Comparative behaviour of Super-Pozz and Dura-Pozz at 28 days without anomalies

CHAPTER 5: CONCLUSION AND RECOMMENDATION

CONCLUSION

This study has been based on samples of two types of classified fly ash marketed by Ash Resources in South Africa (Dura-Pozz: 90% < 45µm and Super-Pozz: 90% < 11µm) used together with a cement sample with chemical composition conforming to the requirements of Class G oil well cement.

These materials were assessed using a comprehensive set of characterisation and analytical techniques, including chemical analysis by XRF, crystal structure determination by X-ray diffraction, microstructure analysis by Scanning Electron Microscopy, proximate analysis by Simultaneous Thermal Analyser (combining TGA and Differential Scanning Calorimetry), particle size analysis by laser diffraction, and pH when added to water.

An investigation of physical and cementing properties formed the focus and objectives of this research, covering:

The first part was to evaluate to the effect of temperature on OWC slurries mixed with different particle sizes of FA and to measure the strength of oil well cement mixed with FA after exposed to high temperatures. The results of this study indicate that, the minimum acceptable compressive strength of 3.45 MPa (500 Psi) according to API that is needed to resist shocks instigated by drilling operations at later stage was reached. From Figure 4.14, it is seen that Dura-Pozz FA increase in strength up to 7.5% addition of FA and recorded a compressive strength of 109 MPa after 28 days at 85 °C. In Figure 4.15, the class G cement samples mixed with 15% Surper-pozz FA proved to have reached a higher compressive strength of 110 MPa after 28 days curing at 85 °C. In Figure 4.16, based on the comparison made between the 2 graphs in terms of compressive strength, Super-Pozz prove to have recorded the highest compressive strength by attaining 110 MPa at 15% FA addition after 28 days.

In the second part of the study, the impact of LSM on the Rheological properties of a cement sample locally supplied by Pretoria Portland Cement (PPC) with similar chemical composition to class oil well cement (viscosity and shear rate) was investigated. The OWC mixed with various LSM dosages were observed at three different temperature. As anticipated, viscosity decreased as the shear rate increased. At 25 ^{0}C and at 45 ^{0}C the rheology behaviour was found to be similar with previous research. Both graphs follow a consistent trend as the viscosity

decreases for the different percentages of LSM ranging from 0.1 % to 0.3%. However, at 60 ^{0}C, the rheology behaviour of 0.7 LSM dosage changed drastically and require further investigation.

The final part of the study involve the investigation of the impact of the various particle sizes of FA on the setting time and flow time of OWC slurries and the cement stability in various environments (offshore/ onshore). As indicated in Figure 4.10, the OWC mixed with FA to a maximum of 30% was found to take significantly longer, 1099 minutes to achieve the 0.0 depth as opposed to the OWC final setting time that was achieved much quicker after 197 minutes.

RECOMMENDATION

It is recommended that further test be conducted on locally and internationally manufactured class G oil well cements to formulate a local substitute mixed with FA for imported cement samples at high temperature (≥ 100°C) in order to revalorise FA. Future work on the following should be investigated:

- The impact of the various particle sizes of FA on the flow time of OWC slurries and the cement stability in various environments (offshore/ onshore) including the evaluation of pressure was not established due to lack of time and equipment. This analysis is recommended for future studies.

- The evaluation of the thickening times of the slurries could not be done at the time when this study was carried out due to time constraint. This evaluation is recommended for future studies.

- The impact of the various particle sizes of FA on the Rheological properties of OWC (Yield stress, plastic viscosity and thixotropic property) could not be established due to time. This analysis is recommended for future studies.
- The comparative effect of temperature on thickening time was not carried out. This evaluation is therefore recommended for future studies.

- A further evaluation into compressive strengths anomalies is therefore recommended for future studies

REFERENCES

Abuhaikal, M.M.A., 2016. *Expansion and shrinkage of early age cementitious materials under saturated conditions: the role of colloidal eigenstresses* (Doctoral dissertation, Massachusetts Institute of Technology).

Ahmaruzzaman, M., 2010. A review on the utilization of fly ash. *Progress in Energy and Combustion Science,* 36(3), p. 327–363.

Allahverdi, A., Kani, E. N. and Soltani, S., 2013. An experimental investigation on improving the medium and late-age compressive strengths of class G oil well cement. *Journal of Petroleum Science and Technology,* 3(1), pp. 01- 07.

Alsop, P. A., 2014. *The Cement Plant Operations Handbook.* Sixth Edition ed. Birmingham : Tradeship Publications Ltd.

API, 2009. *Hydraulic Fracturing Operations-Well Construction and Integrity Guidelines,* Washington: API Publishing Services.

API, 1990. *Specification 10A: Cements and materials for well cementing. 23rd edition.* Washington: American Petroleum Institute.

Apostolidou, C. and Georgakopoulos, A., 2018. *Morphology, Mineralogy, and Chemistry of Fly Ash from the Ptolemais Power Stations, Northern Greece, and its potential as partial Portland cement substitute,* Thessaloniki: Aristotle University of Thessaloniki.

Askar, L. K., Tayeh, B. A. and Bakar, B. A., 2013. Effect of Different Curing Conditions on the Mechanical Properties of UHPFC. *Iranica Journal of Energy and Environment,* 4(3), pp. 299-303.

ASTM C618: Limits of Ash Characterization. *Anonymous Concrete Products*: Denver 116(10), (Oct 2013): 21.

Ayanda, O. S., Fatoki, O. S., Adekola, F. A. and Ximba, B. J., 2012. Characterization of Fly Ash Generated from Matla Power Station in Mpumalanga, South Africa. *E-Journal of Chemistry,* 9(4), pp. 1788-1795.

Bapat, J. D., 2012. *Mineral Admixtures in Cement and Concrete.* 2nd ed. Florida: CRC Press.

Bentz, D. P., 2010. Blending different fineness cements to engineer the properties of cement-based materials. 62(5), pp. 327-338.

Berry, E. and Malhotra, V., 1986. *Fly ash in concrete.* n.d ed. Ottawa: Canadian Government Publishing Centre.

Bogue, R. H., 1929. Calculation of the Compounds in Portland Cement. *Industrial and Engineering Chemistry,* 1(4), pp. 192-197.

Broni-Bediako, E., Joel, O. F. and Ofori-Sarpong, a. G., 2016. Oil Well Cement Additives: A

Review of the Common Types. *Oil Gas Res,* 2 (2), pp. 1-7.
Broni-Bediako, E., Joel, O. and Ofori-Sarpong, G., 2015. Comparative Study of Local Cements with Imported Class 'G' Cement at Different Temperatures for Oil Well Cementing Operations in Ghana. *Petroleum and Environmental,* 6(4), pp. 1-7.
Deng, C.S., Breen, C., Yarwood, J., Habesch, S., Phipps, J., Craster, B. and Maitland, G., 2002. Ageing of oilfield cement at high humidity: a combined FEG-ESEM and Raman microscopic investigation. *Journal of materials chemistry*, *12*(10), pp.3105-3112.

Detwiler, R. J. and Mehta, P. K., 1989. Chemical and physical effects of silica fume on the mechanical behavior of concrete. *ACI Materials Journal,* 86(1), pp. 609-614.
Drexler, D. and Morgan, F. A., 1933. *Method and apparatus for drilling oil wells.* United States, Patent No. US1900163A.
Duguid, A. and Scherer, G. W., 2010. Degradation of oilwell cement due to exposure to carbonated brine. *International Journal of Greenhouse Gas Control,* 4(3), pp. 546-560.
Du Toit, G., van der Merwe, E.M., Kearsley, E.P., McDonald, M. and Kruger, R.A., 2015. Compressive strength of chemically and mechanically activated aluminosilicate systems. In *2015 world of coal ash conference in Nasvhille*.

Earnest, C. M., 1988. *Compositional Analysis by Thermogravimetry,* Philadelphia: American Society for Testing and Materials.
El-Gamal, S., Hashem, F. and Amin, M., 2017. Influence of carbon nanotubes, nanosilica and nanometakaolin on somemorphological-mechanical properties of oil well cement pastessubjected to elevated water curing temperature and regular room aircuring temperature. *Construction and Building Materials,* Volume 146, pp. 531-546.
Goodarzi, F. and Sanei, H., 2009. Plerosphere and its role in reduction of emitted fine fly ash particles from pulverized coal-fired power plants. *Fuel*, *88*(2), pp.382-386.

Faiz Shaikh, S. W. S., 2014. Effect of nano-CaCO3 on compressive strength development of high volume fly ash mortars and concretes. *Journal of Advanced Concrete Technology,* 12(6), pp. 178-186.
Fina, A., Abbenhuis, H.C.L., Tabuani, D., Frache, A. and Camino, G., 2006. Polypropylene metal functionalised POSS nanocomposites: a study by thermogravimetric analysis. *Polymer Degradation and Stability*, *91*(5), pp.1064-1070.

Ghabezloo, S., 2001. Effect of the variations of clinker composition on the poroelastic properties of hardened class G cement paste. *Cement and Concrete Research,* Volume 41, pp.

920-922.
Glossary, 2014. *www.oilgasglossary.com.*Available at: http://oilgasglossary.com [Accessed 26 01 2019].
Heyns, M. and Hassan, M., 2009. *Environmental Effects of Road Pavements Stabilized With Class F Fly Ash,* Bloemfontein: Central University of Technology, Free State.
Ilic, M., Cheeseman, C., Sollars, C. and Knight, J., 2003. Mineralogy and microstructure of sintered lignite coal fly ash. 82(3), pp. 331-336.
Kaduku, T., Daramola, M., Obazu, F. and Iyuke, S., 2015. Synthesis of sodium silicate from South African coal fly ash and its use as an extender in oil well cement applications. *Journal of the Southern African Institute of Mining and Metallurgy,* 115(12), pp. 1175-1182.
Kosmatka, S. H. and Wilson, M. L., 2011. *Design and Control of Concrete Mixtures,* Washignton D.C: Portland Cement Association.
Kruse, K., Jasso, A., Folliard, K., Ferron, R., Juenger, M. and Drimalas, T., 2013. *Characterizing fly ash* (No. FHWA/TX-13/0-6648-1).
Kutchko, B. G. and Kim, A. G., 2006. Fly ash characterization by SEM–EDS. *Fuel,* 85(1), p. 2537–2544.
Labibzadeh, M., Zahabizadeh, B. and Khajehdezfuly, A., 2010. Early-age compressive strength assessment of oil well class G cement due to borehole pressure and temperature changes. *Journal of American Science,* 6(7), pp. 38-47.
Løhre, L. L., 2015. *Revealing the Cause behind Cement Failures by Means of the Knowledge Model of Oil Well Drilling,* Trondheim: Norwegian University of Science and Technology.
Lota, J. S., 1993. *The Hydration of class G oilwell Cement,* London: Royal School of Mines.
Malvern, 2007. *Mastersizer 2000 Essentials.* Worcestershire: s.n.
Matsunaga, T., Kim, J.K., Hardcastle, S. and Rohatgi, P.K., 2002. Crystallinity and selected properties of fly ash particles. *Materials Science and Engineering: A*, *325*(1-2), pp.333-343.
Mc Beath, J. A. M., 2016. *Big oil in the United States: Industry influence on institutions, policy, and politics.* California: Praeger.
Msinjili, N. S. and Schmidt, W. eds., 2015. *Knowledge Exchange for Young Scientists (Keys).* Dar es Salaam Tanzania, BAM Federal Institute for Materials Research and Testing.
Nehdi, S. a., 2012. Rheological properties of oil well cement slurries. *Construction Materials,* 165(CM1), pp. 25-44.
Nelson, E. B. and Guillot, D., 1990. *Well cementing.* 2nd ed. Texas: Schlumberger.
Nmegbu, C., Dagde, K. and Amua, R. U., 2019. The Effect of Temperature on Rheological

Properties of Cement Slurry. *International Journal of Scientific and Engineering Research,* 10(3), pp. 1228-1235.
Obla, K.H., Hill, R.L., Thomas, M.D., Shashiprakash, S.G. and Perebatova, O., 2003. Properties of concrete containing ultra-fine fly ash. *ACI materials journal*, *100*(5), pp.426-433.

Pretorius, I., Piketh, S., Burger, R. and Neomagus, H., 2015. A perspective on South African coal fired power station emissions. *Journal of Energy in Southern Africa,* 26 (3), pp. 27-40.
Ridha, S., Irawan, S. and Ariwahjoedi, B., 2013. Strength prediction of Class G oilwell cement during early ages by electrical conductivity. *Journal of Petroleum Exploration and Production Technology,* 3(4), pp. 303 - 3011.
Salim, P. and Amani, M., 2012. Special considerations in cementing high pressure high temperature wells. *International Journal of Engineering and Applied Sciences,* 1(4), pp. 120-143.
Sancak, E., Sari, Y.D. and Simsek, O., 2008. Effects of elevated temperature on compressive strength and weight loss of the light-weight concrete with silica fume and superplasticizer. *Cement and Concrete Composites*, *30*(8), pp.715-721.

Sankaranarayannan, S. S. and Jagadesan, J. R., 2016. Comparison of High Performance Fly Ash Concrete Using Nano Silica Fume on Different Mixes. *Circuits and Systems,* Volume 7, pp. 1259-1267.
Saout, G. L., Lécolier, E., Rivereau, A. and Zanni, H., 2006. Chemical structure of cement aged at normal and elevated temperatures and pressures: Part I. Class G oilwell cement. *Cement and Concrete Research 36 (2006) 71–78,* 36(1), pp. 71-78.
Satiyawira, B., Fathaddin, M.T. and Setiawan, R., 2010. Effects of lignosulfonate and temperature on compressive strength of cement. In *Proceedings Worl d Geothermal Congress, Bali, Indonesia* (pp. 1-3).
Sedres, G., 2016. *Recovery of SiO2 and Al2O3 from coal fly ash,* Cape Town : University of Western Cape.
Shahria, A. and Nehdi, M. L., 2012. Rheological properties of oil well cement slurries. *Construction Materials,* 165(CM1).
Shahriar, A., 2011. *Investigation on Rheology of Oil Well Cement,* Ontario: University of Western Ontario.
Snellings, R., Mertens, G. and Elsen, J., 2012. Supplementary cementitious materials. *Reviews in Mineralogy and Geochemistry*, *74*(1), pp.211-278.

Soliman, M., Dupont, R., Chapman, B. and Folse, K., 1988. *Case History: 180 Degree Phasing Used in Fracturing of Low Resistivity Zones in Gulf of Mexico Wells,* Houston: Offshore Technology Conference.

Souza, P.P., Soares, R.A., Anjos, M.A., Freitas, J.O., Martinelli, A.E. and Melo, D.F., 2012. Cement slurries of oil wells under high temperature and pressure: the effects of the use of ceramic waste and silica flour. *Brazilian journal of petroleum and gas*, *6*(3).

Stoch, A., 2015. *Fly ash from coal combustion - characterization,* Kraków : KIC InnoEnergy.

Summers, G. R., 2004. A framework for Durable Concrete. *Concrete technology,* 3(1), pp. 22-29.

Sutter, L., 2013. *Methods for Evaluating Fly Ash for Use in Highway Concrete,* Michigan : Michigan Technological University.

Thomas, G. J. J., 2005. US market responds to oil well cement shortages. 103(40), pp. 64-66,68..

Wills, B. A. and Napier-Munn, T., 2006. *Mineral Processing Technology.* Seventh Edition ed. Brisbane: Elsevier Science and Technology Books.

Yahia, A. and Khayat, K.H., 2001. Analytical models for estimating yield stress of high-performance pseudoplastic grout. *Cement and Concrete Research*, *31*(5), pp.731-738.

Yazici, H., 2008. The effect of silica fume and high-volume Class C fly ash on mechanical properties, chloride penetration and freeze–thaw resistance of self-compacting concrete. *Construction and Building Materials,* 22(4), pp. 456-462.

Yazici, Ş. and Arel, H.Ş., 2012. Effects of fly ash fineness on the mechanical properties of concrete. *Sadhana*, *37*(3), pp.389-403.

Yoriya, S., Intana, T. and Tepsri, P., 2019. Separation of Cenospheres from Lignite Fly Ash Using Acetone–Water Mixture. *Applied Science,* 9(18), p. 3792.

Young, A. G., Remmes, B. D. and Meyer, B. J., 1984. Foundation Performance of Offshore Jack-Up Drilling Rigs. *Journal of Geotechnical Engineering,* 110(7), pp. 841-859.

Zhang, J., A.Weissinger, E., Peethamparan, S. and W.Scherer, G., 2010. Early hydration and setting of oil well cement. *Cement and Concrete research, 40(7), pp.1023-1033.,* 40(7), pp. 1023-1033.

Zhou, Z., Sofi, M., Lumantarna, E., San Nicolas, R., Hadi Kusuma, G. and Mendis, P., 2019. Strength Development and Thermogravimetric Investigation of High-Volume Fly Ash Binders. *Materials*, *12*(20), p.3344.

Zulu, S. and Allopi, D., 2016. Evaluating the performance of high-volume fly ash (HVFA) concrete, for South African fly ash. *Invention Journal of Research Technology in Engineering and Management (IJRTEM),* 1(5), pp. 1-7.

APPENDICES

Appendix A: Summary graphs of all FA and the OWC

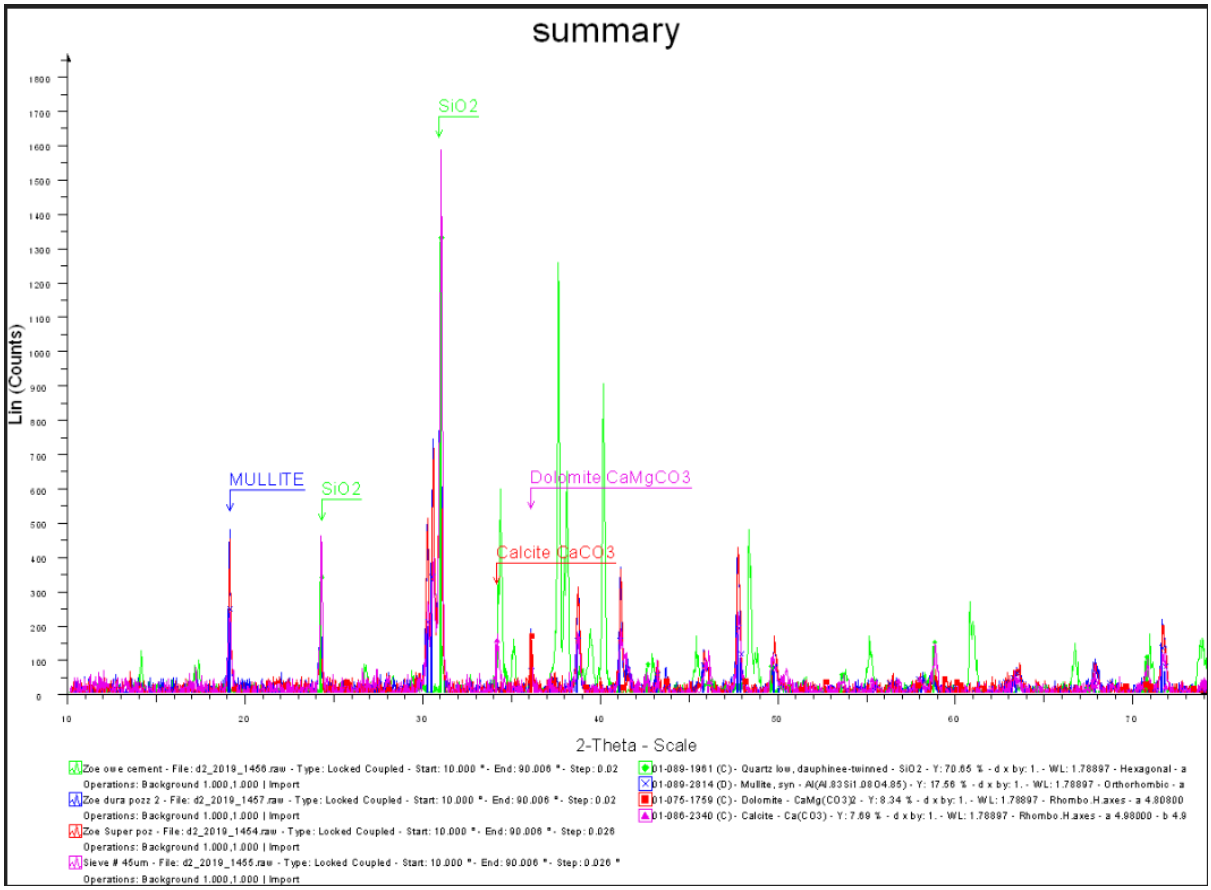

TGA of Dura-Pozz

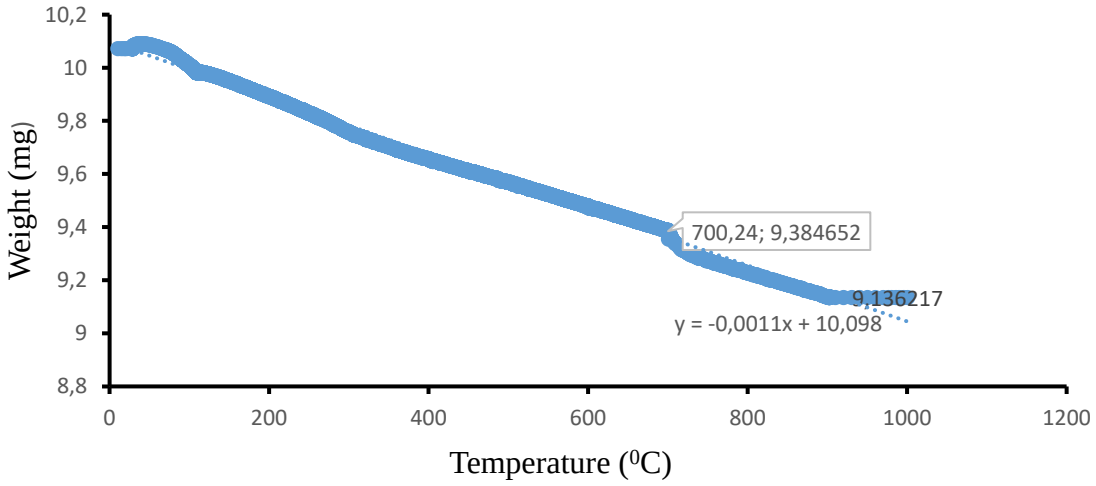

Appendix B: Summary of all compression strength

Dura – Pozz 16 hours compressive test

30 % FA	
Force F (kN)	**Pressure N/mm2**
85.4	53
88.1	55
93.6	59
94.9	59
	Mean 57

Dura – Pozz 2 days compressive test

2.5 % FA	
Force F (kN)	**Pressure N/mm2**
133	83
144,2	90
135,2	84
121,5	76
128,2	80
141	88
	Mean 84

7.5 % FA	
Force F (kN)	**Pressure N/mm2**
142,2	89
133,4	83
140,4	88
151,8	95
146,3	91
144,3	90
	Mean 89

15% FA	
Force F (kN)	**Pressure N/mm2**
137,6	86
125,4	78
140,8	88
139,2	87
134,3	84
131,4	82
	Mean 84

20% FA	
Force F (kN)	**Pressure N/mm2**
141,2	88
119,6	75
135,5	85
132,3	83
115,1	72
135,5	85
	Mean 81

30% FA	
Force F (kN)	**Pressure N/mm2**
137,3	86
164	103
143,7	90
155,1	97
150,9	94
154,2	96
	Mean 94

Dura – Pozz 7 days compressive test

2.5% FA	
Force F (kN)	**Pressure N/mm2**
121,1	80
113,9	71
143,2	90
148,7	93
161,4	101
154,1	96
	Mean 88

7.5% FA	
Force F (kN)	**Pressure N/mm2**
158,6	99
168,6	105
144,9	91
175,5	110
164,7	103
151,6	95
	Mean 100

15% FA	
Force F (kN)	**Pressure N/mm2**
151,7	95
159,1	99
114	71
144,8	91
150,3	94
131,4	95
	Mean 90

20% FA	
Force F (kN)	**Pressure N/mm2**
115,8	72
143,7	90
154,3	96
159,2	99
159,5	100
160	100
	Mean 93

30% FA	
Force F (kN)	**Pressure N/mm2**
149,8	94
160,7	100
181,9	114
125,8	79
173,5	108
185,6	116
	Mean 102

Dura – Pozz 28 days compressive test

2.5% FA	
Force F (kN)	**Pressure N/mm2**
174,4	109
166,6	104
163,5	102
90,8	57
149,1	93
167,5	105
	Mean 95

7.5% FA	
Force F (kN)	**Pressure N/mm2**
171	107
182	114
200	125
121,1	76
	122
	Mean 109

15% FA	
Force F (kN)	**Pressure N/mm2**
122,7	77
155,2	97
142,9	89
131,2	82
132,4	83
140,2	88
	Mean 86

20% FA	
Force F (kN)	**Pressure N/mm2**
155,8	97
164,2	103
166,6	104
165,8	104
176,4	110
165,7	104
	Mean 104

30% FA	
Force F (kN)	**Pressure N/mm2**
148	92
154,7	97
173,8	109
138,4	86
148,8	93
151,5	95
	Mean 95

Super – Pozz 2 days compressive test

2.5% FA	
Force F (kN)	**Pressure N/mm2**
80,6	50
107,2	67
113,7	71
124,4	78
125,5	78
133,2	83
	Mean 71

7.5% FA	
Force F (kN)	**Pressure N/mm2**
117,6	74
120,4	75
126,3	79
134,3	84
135	84
143,7	90
	Mean 81

15% FA	
Force F (kN)	**Pressure N/mm2**
114,5	72
146,4	92
147,7	92
150,6	94
151,3	95
151,7	95
	Mean 90

20% FA	
Force F (kN)	**Pressure N/mm2**
151,5	95
152,3	95
153,5	96
153,6	96
159,2	100
160	100
	Mean 97

30% FA	
Force F (kN)	**Pressure N/mm2**
106,9	67
118,3	74
126,4	79
127,2	79
145	91
152,5	95
	Mean 81

Super – Pozz 7 days compressive test

2.5% FA	
Force F (kN)	**Pressure N/mm2**
135,1	84
146,2	91
114,6	72
141,9	89
149	93
143,3	90
	Mean 86

7.5% FA	
Force F (kN)	**Pressure N/mm2**
151,6	95
165,3	103
147,3	92
150,8	94
164,1	103
141	88
	Mean 96

15% FA	
Force F (kN)	**Pressure N/mm2**
146,2	91
162,9	102
176,8	111
133,5	83
115,9	72
165,7	104
	Mean 94

20% FA	
Force F (kN)	**Pressure N/mm2**
135,2	85
131,3	82
168,9	106
162,1	101
148,9	93
161,4	101
	Mean 95

30% FA	
Force F (kN)	**Pressure N/mm2**
152,2	95
151,2	95
164,3	103
151,8	95
159,9	100
177,4	111
	Mean 100

Super – Pozz 28 days compressive test

2.5% FA	
Force F (kN)	**Pressure N/mm2**
113,9	71
125,5	78
137,4	86
137,3	86
136	85
123	77
	Mean 81

7.5 % FA	
Force F (kN)	**Pressure N/mm2**
173,2	108
163,9	102
143,9	90
169,9	106
153,8	96
163,3	102
	Mean 101

15% FA	
Force F (kN)	**Pressure N/mm2**
175,1	109
182,7	114
154,1	96
173,3	108
175,9	110
193	121
	Mean 110

20% FA	
Force F (kN)	**Pressure N/mm2**
155,8	88
164,2	93
166,6	98
165,8	106
176,4	107
165,7	115
	Mean 101

30% FA	
Force F (kN)	**Pressure N/mm2**
148	90
154,7	110
173,8	83
138,4	95
148,8	100
151,5	109
	Mean 98